ANALYSIS OF COMBINED CONDUCTIVE AND RADIATIVE HEAT TRANSFER IN A TWO DIMENSIONAL SQUARE ENCLOSURE USING THE FINITE VOLUME METHOD

A THESIS SUBMITTED IN PARTIAL FULFILLMENT OF THE REQUIREMENTS FOR THE DEGREE OF

Master of Technology
in
Mechanical Engineering

By

Prabir Kumar Jena

Department of Mechanical Engineering
National Institute of Technology
Rourkela
2009

ANALYSIS OF COMBINED CONDUCTIVE AND RADIATIVE HEAT TRANSFER IN A TWO DIMENSIONAL SQUARE ENCLOSURE USING THE FINITE VOLUME METHOD

A THESIS SUBMITTED IN PARTIAL FULFILLMENT OF THE REQUIREMENTS FOR THE DEGREE OF

Master of Technology
in
Mechanical Engineering

By

Prabir Kumar Jena

Under the guidance of
Prof. Swarup Kumar Mahapatra

Department of Mechanical Engineering
National Institute of Technology
Rourkela
2009

National Institute of Technology
Rourkela

CERTIFICATE

This is to certify that the thesis entitled **"ANALYSIS OF COMBINED CONDUCTIVE AND RADIATIVE HEAT TRANSFER IN A TWO DIMENSIONAL SQUARE ENCLOSURE USING THE FINITE VOLUME METHOD"** submitted by **Mr. Prabir Kumar Jena** in partial fulfillment of the requirements for the award of Master of Technology Degree in **Mechanical Engineering** with specialization in **Thermal Engineering** at the National Institute of Technology, Rourkela (Deemed University) is an authentic work carried out by him under my supervision and guidance.

To the best of my knowledge, the matter embodied in the thesis has not been submitted to any other University/ Institute for the award of any degree or diploma.

Date:

Prof. SWARUP KUMAR MAHAPATRA
Department of Mechanical Engineering
National Institute of Technology
Rourkela – 769008

CONTENTS

CERTIFICATE i

CONTENTS ii

ACKNOWLEDGEMENT iv

ABSTRACT v

LIST OF FIGURES vi

LIST OF TABLES viii

NOMENCLATURE ix

CHAPTERS

1. INTRODUCTION AND LITERATURE REVIEW 1

2. DISCRETIZATION METHODS BY USING FVM

2.1 The nature of numerical methods 6

2.1.1 The discretization concept 6

2.1.2 The structure of the discretization equation 7

2.2 Methods of deriving the discretization equations 7

2.3 Control-volume formulation 8

2.3.1 Finite volume: basic methodology 9

2.3.2 Cells and nodes 9

2.4 Finite volume method for unsteady flows 11

2.4.1 One-dimensional unsteady heat conduction 11

2.4.2 Explicit scheme 13

2.4.3 The fully implicit scheme 14

2.4.4 Crank-Nicholson scheme 15

2.5 Two-dimensional unsteady heat conduction 16

2.6 Solutions of algebraic equations 20

2.6.1 The Tri-diagonal matrix algorithm 21

2.7 Computational domain 23

2.8 Flow chart for solving transient conduction 23

3. RADIATIVE HEAT TRANSFER

3.1 Mathematical description of radiation 25

3.2 Radiative properties of materials 26

3.2.1 Black body radiation 26

3.2.2 Surface properties 27

3.3 Formulation of RTE by using FV method 28

3.4 Solution Procedure 34

4. ANALYSIS

4.1 Energy equation 36

4.2 Calculation of incident radiation and heat flux 36

5. RESULTS AND DISCUSSION 39

6. CONCLUSIONS AND FUTURE SCOPE

6.1 CONCLUSIONS 57

6.2 FUTURE SCOPE 57

7. LIST OF REFERENCES 59

ACKNOWLEDGEMENT

I am extremely fortunate to be involved in an exciting and challenging research project like "analysis of combined conductive and radiative heat transfer in a two dimensional square enclosure using the finite volume method". This project increased my thinking and understanding capability as I started the project from scratch.

I would like to express my greatest gratitude and respect to my supervisor Prof. Swarup Kumar Mahapatra, for his excellent guidance, valuable suggestions and endless support. He has not only been a wonderful supervisor but also a genuine person. I consider myself extremely lucky to be able to work under guidance of such a dynamic personality. Actually he is one of such genuine person for whom my words will not be enough to express.

I would like to express my sincere thanks to Prof. R.K.Sahoo for his precious suggestions and encouragement to perform the project work. He was very patient to hear my problems that I am facing during the project work and finding the solutions. I am very much thankful to him for giving his valuable time for me.

I would like to express my thanks to all my classmates, all staffs and faculty members of mechanical engineering department for making my stay in N.I.T. Rourkela a pleasant and memorable experience and also giving me absolute working environment where I unlashed my potential .

I want to convey my heartiest gratitude to my parents for their unfathomable encouragement.

Date:

Prabir Kumar Jena
Roll. No. 207ME310
M.Tech. (Thermal)

Abstract

An efficient tool to deal with multidimensional radiative heat transfer is in strong demand to analyse the various thermal problems combined either with other modes of heat transfer or with combustion phenomena. Combined conduction and radiation heat transfer without heat generation is investigated. Analysis is carried out for both steady and unsteady situations. Two-dimensional gray Cartesian enclosure with an absorbing, emitting, and isotropically scattering medium is considered. Enclosure boundaries are assumed at specified temperature. The finite volume method is used to solve the energy equation and the finite volume method is used to compute the radiative information required in the solution of energy equation. The Implicit scheme is used to solve the transient energy equation. Transient and steady state temperature and heat flux distributions are found for various radiative parameters.

In the last two decade, finite volume method (FVM) emerged as one of the most attractive method for modeling steady as well as transient state radiative transfer. The finite volume method is a method for representing and evaluating partial differential equations as algebraic equations. Similar to the finite difference method, values are calculated at discrete places on a meshed geometry. "Finite volume" refers to the small volume surrounding each node point on a mesh. In the finite volume method, volume integrals in a partial differential equation that contain a divergence term are converted to surface integral using divergence theorem. These terms are then evaluated as fluxes at the surfaces of each finite volume. Because the flux entering a given volume is identical to that leaving the adjacent volume, these methods are conservative.

In the present work the boundaries are assumed to be gray and the medium scatters isotropically. The current study examines the finite volume method (**FVM**) for coupled radiative and conductive heat transfer in square enclosures in which either a non-scattering or scattering medium is included**. Implicit Scheme** has been used for solving the coupled conductive and radiative heat transfer equation. The transient temperature distributions are studied for the effects of various parameters like the extinction coefficient, the scattering albedo and the conduction radiation parameter for both constant. The effect of radiative parameters on the system to reach the steady state is also studied.

LIST OF FIGURES

Figure No.	Title	Page No.
2.1	Three successive grid points used for the Taylor-series expansion	8
2.2	Cells and Nodes of Control Volume	10
2.3	Typical Control Volume	10
2.4	One dimensional control volume	11
2.5	Two Dimensional Control Volume	17
2.6	Computational Domain	23
3.1	Typical control angle	30
3.2	Intensity I^l in direction $\Delta\Omega^l$ in the center of the elemental Sub-solid angle Ω^l	30
3.3	Control angle orientations	32
3.4	Flowchart for overall solution procedure	34
5.1	Temperature isotherms at steady state	39
5.2	Variation of Heat flux at the bottom wall along X-axis	40
5.3	Variation of heat flux at the top cold wall along X-axis	40
5.4	Variation of heat flux at the side cold wall along Y-axis	41
5.5	Dimensionless temperature profiles for N=1	42
5.6	Dimensionless temperature profiles for N=0.1	42
5.7	Dimensionless temperature profiles for N=0.01	43
5.8	Dimensionless temperature profiles for N=0.001	43
5.9	Variation of fractional radiative heat flux for N=1	44
5.10	Variation of fractional radiative heat flux for N=0.1	45
5.11	Variation of fractional radiative heat flux for N=0.01	46
5.12	Variation of fractional radiative heat flux for N=0.001	47
5.13	Variation of the total heat flux for wall emissivity of ε_w=1 at the bottom	48
5.14	Variation of total heat flux for ε_w=0.8, at the bottom wall, Y=0.	48
5.15	Variation of total heat flux for ε_w=0.5, at the bottom wall, Y=0	49
5.16	Variation of total heat flux for ε_w=0.2, at the bottom wall, Y=0.	49
5.17	Temperature isotherms for N=0.001 and ω=0.	50

LIST OF FIGURES

Figure No.	Title	Page No.
5.18	Temperature isotherms for N=0.001 and ω=0.5.	51
5.19	Temperature isotherms for N=0.001 and ω=1.	51
5.20	Temperature isotherms for N=0.001 and ω=0 and ε=0.5.	52
5.21	Temperature isotherms for N=0.001 and ω=0.5 and ε=0.5.	52
5.22	Number of time steps = 20.	53
5.23	Number of time steps=40.	53
5.24	Number of time steps=80.	54
5.25	Temperature Variation with time	54

LIST OF TABLES

Table No.	Title	Page No.
5.1	Variation in time period required to reach at steady state.	55

NOMENCLATURE

K	Thermal conductivity
N	Conduction-Radiation parameter
ρ	Density of the medium
q_r	Radiative heat flux
q_c	Conductive heat flux
a	coefficient of discretization equation
b	source term in discretization equation
c	the speed of light
D'_{cx}, D'_{cy}	direction cosine in x , y direction respectively
G	incident radiation
I	actual intensity
M	total number of control angels
$\hat{n}$	unit outward normal vector of the control volume face
q	heat flux
s	distance
S	source function
S_m^l	modified source function
$\hat{s}$	unit direction vector
T	temperature
t	time
ζ	Non-dimensional time
x, y, z	coordinate direction
β	extinction coefficient
β_m^l	modified extinction coefficient
ΔA	area of control volume faces

Δv	volume of control volume
$\Delta x, \Delta y$	x and y direction control volume width
$\Delta\Omega$	control angle
ε	emissivity
θ	polar angle measured from $\hat{e}_z$
κ	absorption coefficient
σ_s	scattering coefficient
σ	Stefan-Boltzmann's coefficient
Φ	scattering phase function
$\Phi^{l'l}$	average scattering phase function
ϕ	azimuthal angle measured from $\hat{e}_x$

Subscripts

b	black body
D	downstream
m	modified
P	node
U	upstream
E, W, N, S	east, west, north, south neighbors of *P*
e, w, n, s	east, west, north, south direction

superscripts

l, l'	angular directions
0	value from previous iteration
*	non-dimensional quantities

CHAPTER 1

INTRODUCTION AND LITERATURE REVIEW

INTRODUCTION AND LITERATURE REVIEW

Efficiency improvements in most industrial thermal processes are achieved by increased process temperatures. The optimum design of such processes is leading to temperature loads near the existing material limits. In recent years, high-temperature-resistant materials, made not only of ceramics but also of special alloys, have become available to realize high-temperature furnaces, gas turbine combustion chambers and blades, heat exchangers, porous volumetric solar receivers, surface and porous IR-radiant burners. Experimental and numerical investigations are necessary in order to perform an optimum design and to elucidate the advantages of the temperature increase of such improved processes utilizing advanced high-temperature materials. Numerical computations of flow with heat and mass transfer in such high-temperature appliances require a through consideration of radiative heat transfer.

Radiation either combined with other modes of heat transfer or with combustion phenomena in a multidimensional enclosure such as a combustion chamber, furnace and porous medium has received much attention due to a realization of its importance in the associated application fields. However, since an exact analytical solution to the highly non-linear integro differential radiative transfer equation (RTE) is nearly impossible to find, an efficient tool to deal with multidimensional radiative heat transfer is in strong demand to analyse various thermal problems.

Analysis of combined conduction and radiation heat transfer in a radiatively participating medium has numerous engineering applications. Examples of such applications are in the analysis of heat transfer through high temperature energy conversion devices, semitransparent materials, fibrous and foam insulations, porous materials, and so on. In recent years, a good amount of work has been reported in the area of steady [1-5] and unsteady [6-12] combined conduction-radiation problems in an absorbing, emitting, and scattering medium. Although most of the steady state studies were associated with temperature boundary conditions, some of the papers discussed the problems with flux boundary conditions. Tan and Lallemand [13] examined the transient temperature distribution in a glass plate subjected to various boundary conditions. The transient heating of an absorbing, emitting, and scattering material with different black plate boundary conditions was studied by Yuen and Khatami [14]. They used a semi-explicit finite-difference scheme to generate numerical solutions. For solving the transient energy equation, Tsai and Lin [15] used the Crank-Nicholson scheme and the radiative part was solved by the nodal

approximation technique. Tong et al. [16] analyzed transient radiation heat transfer through semi-isotropic scattering planar porous materials. They solved the radiative part using a two-flux model.

The transient cooling problem with isotropic scattering in a cylindrical geometry was analyzed by Baek et al. [17]. For solving the radiative part, they used the discrete ordinate method, and a finite difference scheme was used to solve the transient energy equation. Tsai and Nixon [18] considered a multilayered geometry without the effect of isotropic scattering. Hahn et al. [19] examined the transient heat transfer using a multiflux model to solve the radiative part. They analyzed the transient state of heat transfer in a layer of ceramic powder during laser flash measurements of thermal diffusivity. Here also the effect of scattering was not included. The problem with the melting of a semitransparent slab by an external radiating source was investigated by Diaz and Viskanta [20]. A similar problem was also studied by Seki and Nishimura et al. [21] Matthews et al. [22] discussed the steady and unsteady combined conduction-radiation heat transfer heated by a highly concentrated solar radiation. A two-flux model was used to solve the radiative part. Transient cooling of a semitransparent material was examined by Siegel [10]. A finite difference procedure was adopted to obtain a highly accurate temperature distribution across the layer. Yao and Chung [11] solved a similar type of problem using an implicit finite volume scheme. The integral equation for radiative heat flux was solved by a singularity subtraction technique and Gaussian quadrature. Recently, studies related to this subject have been reviewed in detail by Siegel.

Although in the past decades a variety of computational schemes have been developed to obtain an approximate solution to RTE, each scheme has demerits as well as merits in its application. Techniques formerly used to solve RTE include the Eddington and Schuster-Schwarzchild [23]. Even if the Monte Carlo [24] and zone methods [25] are called exact numerical solutions, the former consumes an excessively large computational time and the latter is not easily applicable to analyzing a radiatively scattering medium. Furthermore, most of the methods previously adopted to solve RTE are incompatible with the finite difference algorithm used in solving the continuity, momentum and energy equations which are involved in various thermal and fluid mechanical problems

Numerical computations of radiation based on conventional methods such as the zonal method, the Monte Carlo method (MCM), etc., prove to be laborious and very time consuming. For this reason, numerous investigations [2–4] are currently being carried out worldwide to assess computationally efficient methods.

Numerical simulations of the high-temperature appliances mentioned above require multi-dimensional analysis. Treatment of radiative transport in the multidimensional geometry is difficult mainly because of the three extra independent variables namely the polar angle, the azimuthal angle and the wavelength. Since there is no way out to get rid of the physical dimensions of the geometry and the wavelength of radiation, all numerical models, except the zonal method and the MCM, deal with different types of discretization schemes to make radiation less and less dependent on angular dimensions. The various methods differ primarily in the angular discretization schemes and the use of either the differential form or the integral form of the radiative transfer equation. The finite element method for the calculation of a coupled conductive and radiative heat transfer problem in two-dimensional rectangular enclosures [26]. However it was found to be not only time consuming, but also difficult to apply to a scattering medium.

The main objective behind the development of any method for the solution of radiative transport problems, apart from its versatility for various geometries, complex medium conditions, etc., is that the method should be computationally efficient.

The finite volume method (FVM) for radiation is a robust method. It has many advantages over other numerical methods such as the PN approximation, discrete transfer method and the discrete ordinate method.

The present study examines the FVM for a coupled conductive and radiative heat transfer in a two-dimensional square enclosure. In this work the conductive term is discretized using the central differencing scheme and FVM approximation is adopted to model the term of divergence of radiative heat flux in the energy equation. The solutions will be presented using isothermal contours, radiative and total heat fluxes and transient behavior of temperature for easy understanding of the phenomena involved.

CHAPTER 2

DISCRETIZATION METHODS BY USING FVM

2. DISCRETIZATION METHODS BY USING FVM:

2.1 THE NATURE OF NUMERICAL METHODS:

A numerical solution of a differential consists of a set of numbers from which the distribution of the dependent variable ϕ can be constructed.

Let us suppose that we decide to represent the variation of ϕ by a polynomial in x,

$$\phi = a_0 + a_1 x + a_2 x^2 + ... + a_m x^m \tag{2.1}$$

and employ a numerical method to find the finite number of coefficients $a_0, a_1, a_2, ..., a_m$. This will enable us to evaluate ϕ at any location x by substituting the value of x and the values of the *a's* into equation (2.1). This procedure is, however, somewhat inconvenient if our ultimate interest is to obtain the value of ϕ at various locations.

Therefore, we should think for a numerical method, which treats as its basic unknowns the values of the dependent variable at a finite number of locations (called the *grid points*) in the calculation domain.

2.1.1 The Discretization Concept:

Now we have replaced the continuous information contained in the exact solution of the differential equation with discrete values by focusing our attention on the values at the grid points. We have thus discretized the distribution ofϕ, and it is appropriate to refer to this class of numerical methods as *discretization methods*.

The algebraic equations involving the unknown values of ϕ at chosen grid points, which we shall now name the *discretization equations,* are derived from the differential equation governingϕ. In this derivation, we must employ some assumption about how ϕ varies between the grid points. Although this "profile" of ϕ could be chosen such that a single algebraic expression suffices for the whole calculation domain, it is often more practical to use piecewise profile such that a given segment describes the variation of ϕ over only a small region in terms of ϕ values at the grid points within and around that region. Thus, it is common to subdivide the calculation domain into a number of sub domains or elements such that a separate profile assumption can be associated with each sub domain.

In the discretization concept the continuum calculation domain has been discretized. It is this systematic discretization of space and of the dependent variables that makes it possible to replace the governing differential equation with simple algebraic equations, which can be solved with relative ease.

2.1.2 The Structure of the Discretization Equation:

A discretization equation is an algebraic relation connecting the values of ϕ for a group of grid points. Such an equation is derived from the differential equation governing ϕ and thus expresses the same physical information as the differential equation. That only a few grid points participate in a given discretization equation is a consequence of the piecewise nature of the profiles chosen. The value of ϕ at a grid point thereby influences the distribution of ϕ only in its immediate neighborhood. As the number of grid points becomes very large, the solution of the discretization equations is expected to approach the exact solution of the corresponding differential equation. This follows from the consideration that, as the grid points get closer together, the change in ϕ between neighboring grid points becomes small, and then the actual details of the profile assumption become unimportant.

2.2 METHODS OF DERIVING THE DISCRETIZATION EQUATIONS:

For a given differential equation, the required discretization equations can be derived in many ways and Taylor-Series formulation is one of them.

Taylor-Series Formulation:

The usual procedure for deriving finite-difference equation consists of approximating the derivatives in the differential equation via a truncated Taylor series. Let us consider the grid points in fig (2.1). For grid point 2, located midway between grid points 1 and 3 such that

$\Delta x = x_2 - x_1 = x_3 - x_2$, the Taylor-series expansion around 2 gives

$$\phi_1 = \phi_2 - \Delta x\left(\frac{d\phi}{dx_2}\right) + \frac{1}{2}(\Delta x)^2\left(\frac{d^2\phi}{dx^2}\right)_2 - \ldots\ldots\ldots\ldots \quad (2.2)$$

$$\phi_3 = \phi_2 + \Delta x\left(\frac{d\phi}{dx}\right)_2 + \frac{1}{2}(\Delta x)^2\left(\frac{d^2\phi}{dx^2}\right)_2 + \text{.....} \tag{2.3}$$

Truncating the series just after the third term, and adding and subtracting the two equations, we obtain

$$\left(\frac{d\phi}{dx}\right)_2 = \frac{\phi_3 - \phi_1}{2\Delta x} \tag{2.4}$$

$$\left(\frac{d^2\phi}{dx^2}\right)_2 = \frac{\phi_1 - 2\phi_2 + \phi_3}{(\Delta x)^2} \tag{2.5}$$

The substitution of such expression into the differential equation leads to the finite-difference equation.

The method includes the assumption that the variation of ϕ is somewhat like a polynomial in x, so that the higher derivatives are unimportant. This assumption, however, leads to an undesirable formulation when, for example, exponential variations are encountered.

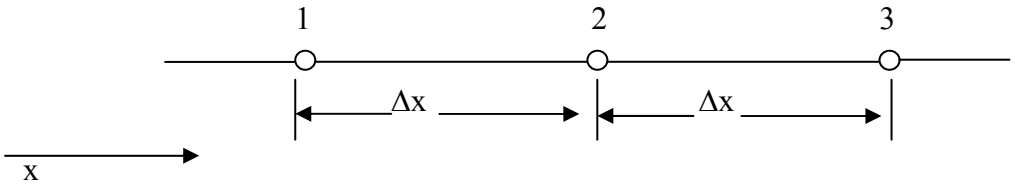

Figure 2.1 Three successive grid points used for the Taylor-series expansion.

2.3 CONTROL-VOLUME FORMULATION

The Finite Volume Method (FVM) is one of the most versatile discretization techniques used in CFD. Based on the control volume formulation of analytical fluid dynamics, the first step in the FVM is to divide the domain into a number of control volumes (aka cells, elements) where the variable of interest is located at the centroid of the control volume. The next step is to integrate the differential form of the governing equations (very similar to the control volume approach) over each control volume. Interpolation profiles are then assumed in order to describe the variation of the concerned variable between cell centroids. The resulting equation is called the discretized or discretization equation. In this manner, the discretization equation expresses the conservation principle for the variable inside the control volume.

The most attractive features of the control-volume formulation is that the resulting solution would imply that the *integral* conservation of quantities such as mass, momentum, and energy is exactly satisfied over any group of control volumes and over the whole calculation domain. Even a coarse grid solution exhibits exact integral balances.

Advantages: (1) Basic FV control volume balance does not limit cell shape.

(2)Mass, Momentum, Energy conserved even on coarse grids.

(3)Efficient, iterative solvers well developed.

(4) FVM enjoys an advantage in memory use and speed for very large problems, higher speed flows, turbulent flows, and source term dominated flows (like combustion).

2.3.1 Finite Volume: Basic Methodology

(1)Divide the domain into control volumes.

(2)Integrate the differential equation over the control volume and apply the divergence theorem.

(3)To evaluate derivative terms, values at the control volume faces are needed: have to make an assumption about how the value varies.

(4)Result is a set of linear algebraic equations: one for each control volume.

(5)Solve iteratively or simultaneously.

2.3.2 Cells and Nodes

(1)Using finite volume method, the solution domain is subdivided into a finite number of small control volumes (cells) by a grid.

(2)The grid defines the boundaries of the control volumes while the computational node lies at the center of the control volume.

(3)The advantage of FVM is that the integral conservation is satisfied exactly over the control volume.

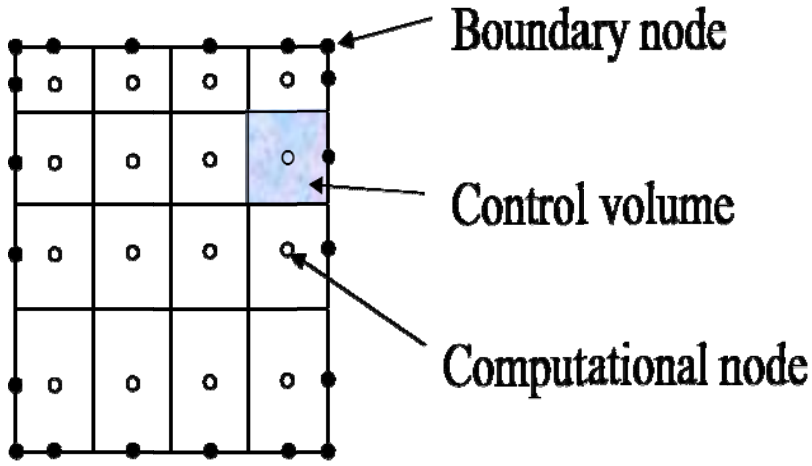

Figure 2.2 Cells and Nodes of Control Volume

Typical Control volume

(1)The net flux through the control volume boundary is the sum of integrals over the four control volume faces (six in 3D). The control volumes do not overlap.

(2)The value of the integrand is not available at the control volume faces and is determined by interpolation.

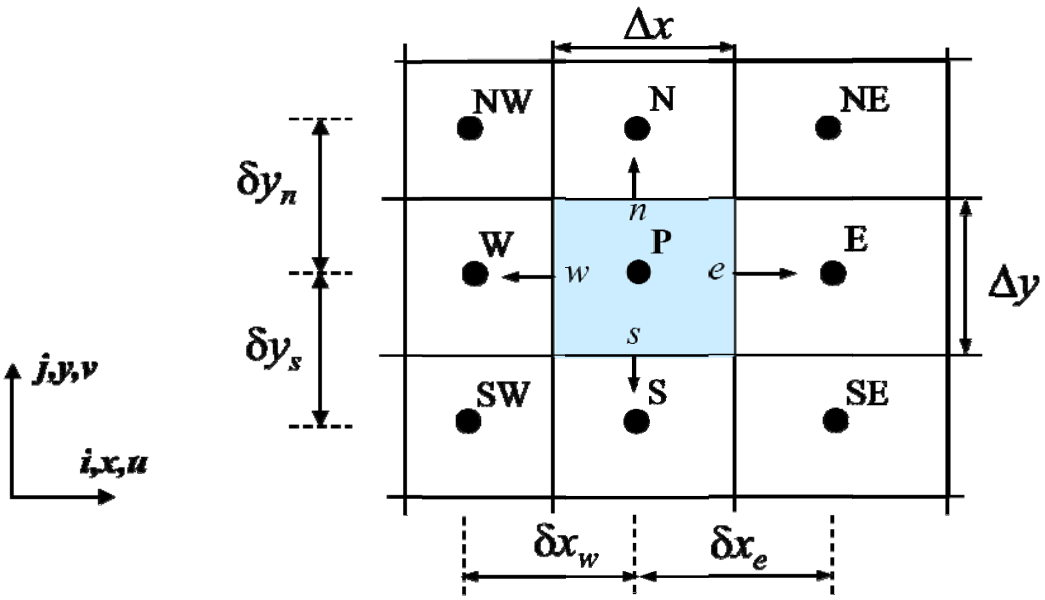

Figure 2.3 Typical Control Volume

2.4 FINITE VOLUME METHOD FOR UNSTEADY FLOWS:

2.4.1 ONE-DIMENSIONAL UNSTEADY HEAT CONDUCTION:

Unsteady one-dimensional heat conduction is governed by the equation

$$\rho c\frac{\partial T}{\partial t}=\frac{\partial}{\partial x}(K\frac{\partial T}{\partial x})+S \tag{2.6}$$

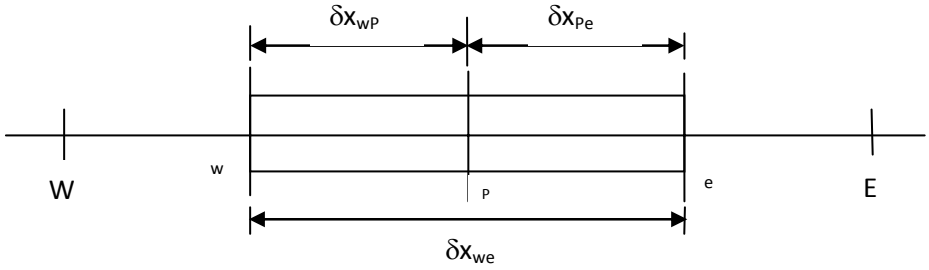

Figure 2.4 One dimensional control volume

Consider the one-dimensional control volume in Figure-2.4 Integration of equation over the control volume and over a time interval from t to t+Δt gives

$$\int_t^{t+\Delta t}\int_{CV}\rho c\frac{\partial T}{\partial t}dVdt=\int_t^{t+\Delta t}\int_{CV}\frac{\partial}{\partial x}(K\frac{\partial T}{\partial x})dVdt+\int_t^{t+\Delta t}\int_{CV}sdVdt \tag{2.7}$$

This may be written as

$$\int_w^e\left[\int_t^{t+\Delta t}\rho c\frac{\partial T}{\partial t}dt\right]dV=\int_t^{t+\Delta t}\left[\left(KA\frac{\partial T}{\partial x}\right)_e-\left(KA\frac{\partial T}{\partial x}\right)_w\right]dt+\int_t^{t+\Delta t}\bar{S}\Delta Vdt \tag{2.8}$$

In equation A is the face area of the control volume,ΔV is its volume, which is equal to AΔx where Δx is the width of the control volume and $\bar{S}$ is the average source strength.If the temperature at a node is assumed to prevail over the whole control volume,the left hand side can be written as

$$\int_{CV}\left[\int_t^{t+\Delta t}\rho c\frac{\partial T}{\partial t}dt\right]dV=\rho c\left(T_P-T_P{}^o\right)\Delta V \tag{2.9}$$

In equation (2.9) superscript '*o*' refers to temperature at time *t*; temperatures at time level t+Δt are not superscripted. The same result as (2.9) would be obtained by substituting $\left(T_P-T_P{}^o\right)\Big/\Delta t$ for $\frac{\partial T}{\partial t}$ so this term has been discretised using a first (backward) differencing

scheme. If we apply central differencing schemes to the diffusion terms on the right hand side equation (2.8) may be written as

$$\rho c\left(T_P - T_P^{\,o}\right)\Delta V = \int_t^{t+\Delta t}\left[\left(K_e A\frac{T_E - T_P}{\delta x_{PE}}\right) - \left(K_w A\frac{T_P - T_W}{\delta x_{WP}}\right)\right]dt + \int_t^{t+\Delta t}\bar{S}\Delta V dt \qquad (2.10)$$

To evaluate the right hand side of this equation we need to make an assumption about the variation of T_P, T_E and T_W with time. We could use temperatures at time t or at time $t+\Delta t$ to calculate the time integral or, alternatively, a combination of temperatures at time $t+\Delta t$. We may generalize the approach by means of a weighing parameter θ between 0 and 1 and write the integral I_T of temperature T_P with respect to time as

$$I_T = \int_t^{t+\Delta t} T_P dt = \left[\theta T_P + (1-\theta)T_P^{\,o}\right]\Delta t \qquad (2.11)$$

Hence

θ	0	1/2	1
I_T	$T_P^{\,0}\Delta t$	$\frac{1}{2}\left(T_P + T_P^{\,o}\right)\Delta t$	$T_P\Delta t$

If θ=0 the temperature at (old) time level t is used; if θ=1 the temperature at new time level $t+\Delta t$ is used; and finally if θ=1/2, the temperature at t and $t+\Delta t$ are equally weighed.

Using formula (2.11) for T_W and T_E in equation (2.10), and dividing by $A\Delta t$ throughout, we have

$$\rho c\left(\frac{T_P - T_P^{\,o}}{\Delta t}\right)\Delta x = \theta\left[\frac{K_e(T_E - T_P)}{\delta x_{PE}} - \frac{K_w(T_P - T_W)}{\delta x_{WP}}\right]$$

$$+ (1-\theta)\left[\frac{K_e\left(T_E^{\,o} - T_P^{\,o}\right)}{\delta x_{PE}} - \frac{K_w\left(T_P^{\,o} - T_W^{\,o}\right)}{\delta x_{WP}}\right] + \bar{S}\Delta x \qquad (2.12)$$

This may be re-arranged to give

$$\left[\rho c\frac{\Delta x}{\Delta t}+\theta\left(\frac{K_e}{\delta x_{PE}}+\frac{K_w}{\delta x_{WP}}\right)\right]T_P=\frac{K_e}{\delta x_{PE}}\left[\theta T_E+(1-\theta)T_E{}^o\right]+\frac{K_w}{\delta x_{WP}}\left[\theta T_W+(1-\theta)T_W{}^o\right]+$$

$$\left[\rho c\frac{\Delta x}{\Delta t}-(1-\theta)\frac{K_e}{\delta x_{PE}}-(1-\theta)\frac{K_w}{\delta x_{WP}}\right]T_P{}^o+\bar{S}\Delta x \qquad (2.13)$$

Now we identify the coefficients of T_W and T_E as a_W and a_E and write equation (2.13) in the familiar standard form:

$$a_PT_P=a_W\left[\theta T_W+(1-\theta)T_W{}^o\right]+a_E\left[\theta T_E+(1-\theta)T_E{}^o\right]+\left[a_P{}^o-(1-\theta)a_W-(1-\theta)a_E\right]T_P{}^o+b \qquad (2.14)$$

Where $a_P=\theta(a_W+a_E)+a_P{}^o$

And $a_P{}^o=\rho c\frac{\Delta x}{\Delta t}$

With

a_W	a_E	b
$\frac{K_w}{\delta x_{WP}}$	$\frac{K_e}{\delta x_{PE}}$	$\bar{S}\Delta x$

The exact form of the final discretised equation depends on the value of θ. When θ is zero, we only use temperatures $T_P{}^o, T_W{}^o \text{ and } T_E{}^o$ at the old time level t on the right hand side of equation (2.14) to evaluate T_P at the new time; the resulting scheme is called **explicit**. When $0<\theta<1$ temperatures at the new time level are used on the both sides of the equation; the resulting schemes are called **implicit.** The extreme case of $\theta=1$ is termed **fully implicit** and the case corresponding to $\theta=1/2$ is called the **Crank-Nicolson scheme.**

2.4.2 EXPLICIT SCHEME:

In the explicit scheme the source term is linearised as $b=S_u+S_pT_p{}^o$. Now the substitution of $\theta=0$ into (2.14) gives the explicit discretisation of the unsteady conductive heat transfer equation:

$$a_P T_P = a_W T_W{}^o + a_E T_E{}^o + \left[a_P{}^o - (a_W + a_E - S_p)\right] T_P{}^o + S_u \tag{2.15}$$

$$a_P = a_P{}^o$$

$$a_P{}^o = \rho c \frac{\Delta x}{\Delta t}$$

$$a_W = \frac{K_w}{\delta x_{WP}}$$

$$a_E = \frac{K_e}{\delta x_{PE}}$$

The right side of equation (2.15) only contains values at the old time step so the left hand side can be calculated by forward marching in time. The scheme is based on backward differencing and its Taylor series truncation error accuracy is first-order with respect to time. All the coefficients need to be positive in the discretised equation. The coefficients of $T_P{}^o$ may be viewed as the neighbor coefficient connecting the values at the old time level to those at the new time level. For this coefficient to be positive we must have $a_P{}^o - a_W - a_E > 0$. For constant K and uniform grid spacing, $\delta x_{PE} = \delta x_{WP} = \Delta x$, this may be written as

$\rho c \frac{\Delta x}{\Delta t} \succ \frac{2K}{\Delta x}$ or we can write

$$\Delta t \prec \rho c \frac{(\Delta x)^2}{2K}$$

This inequality sets a stringent maximum limit to the time step size and represents a serious limitation for the explicit scheme. It becomes very expensive to improve spatial accuracy because the maximum possible time step needs to be reduced as the square of Δx. Consequently, this method is not recommended for general transient problems.

2.4.3 THE FULLY IMPLICIT SCHEME:

When the value of θ is set equal to 1 we obtain the fully implicit scheme. The discretised equation is

$$a_P T_P = a_W T_W + a_E T_E + a_P{}^o T_P{}^o + S_u \tag{2.16}$$

Where $a_P = a_P^{\,o} + a_W + a_E - S_P$

and $a_P^{\,o} = \rho c \dfrac{\Delta x}{\Delta t}$

with $a_W = \dfrac{K_w}{\delta x_{WP}}$

$a_E = \dfrac{K_e}{\delta x_{PE}}$

Both sides of the equation contain temperatures at the new time step, and a system of algebraic equation must be solved at each time step. The time marching procedure starts with a given initial field of temperatures T^o. The system of equations (2.16) is solved after selecting time step Δt. Next the solution T is assigned to T^o and the procedure is repeated to progress the solution by a further time step.

It can be seen that all the coefficients are positive, which makes the implicit scheme unconditionally stable for any size of time step. The implicit method is recommended for general purpose transient calculation because of its robustness and unconditional stability.

2.4.4 CRANK-NICOLSON SCHEME:

The Crank-Nicolson scheme method results from setting θ=1/2 in equation (2.14) . Now the discretised unsteady heat conduction equation is

$$a_P T_P = a_E \left[\frac{T_E + T_E^{\,o}}{2} \right] + a_W \left[\frac{T_W + T_W^{\,o}}{2} \right] + \left[a_p^{\,o} - \frac{a_E}{2} - \frac{a_W}{2} \right] T_P^{\,o} + b \qquad (2.17)$$

Where $a_P = \dfrac{1}{2}\left(a_W + a_E\right) + a_P^{\,o} - \dfrac{1}{2} S_P$

And $a_P^{\,o} = \rho c \dfrac{\Delta x}{\Delta t}$

a_W	a_E	b
$\dfrac{K_w}{\delta x_{WP}}$	$\dfrac{K_e}{\delta x_{PE}}$	$S_u + \dfrac{1}{2} S_P T_P^{\,o}$

Since more than one unknown value of T at the new time level is present in equation (2.17) the method is implicit and simultaneous equations for all node points need to be solved at each time step. Although schemes with $1/2 \leq \theta \leq 1$, including the Crank-Nicolson scheme, are unconditionally stable for all values of the time step. It is more important to ensure that all the coefficients are positive for physically realistic and bounded results. This is the case if the coefficients of T_P^o satisfies the following condition:

$$a_P{}^o \succ \left[\frac{a_E + a_W}{2}\right]$$

Which leads to

$$\Delta t \prec \rho c \frac{\Delta x^2}{K}$$

This time step limitation is only slightly less restrictive than associated with the explicit method. The Crank-Nicolson method is based on central differencing and hence it is the second-order accurate in time. With sufficiently small time steps it is possible to achieve considerably greater accuracy than with the explicit method. The overall accuracy of a computation depends upon on the spatial differencing practice, so the Crank-Nicolson scheme is normally used in conjunction with spatial central differencing.

2.5 TWO-DIMENSIONAL UNSTEADY HEAT CONDUCTION:

A portion of a two-dimensional grid is shown in fig-2.5.For the grid point P, points E and W are its x-direction neighbors, while N and S (denoting north and south) are the y-direction neighbors. The control volume around P is shown by dashed lines. Its thickness in z direction is assumed to be unity. The actual location of the control volume faces in relation to the grid points is exactly midway between the neighboring grid points.

$$\rho c \frac{\partial T}{\partial t} = \frac{\partial}{\partial x}(K \frac{\partial T}{\partial x}) + \frac{\partial}{\partial y}(K \frac{\partial T}{\partial y}) + S \qquad (2.18)$$

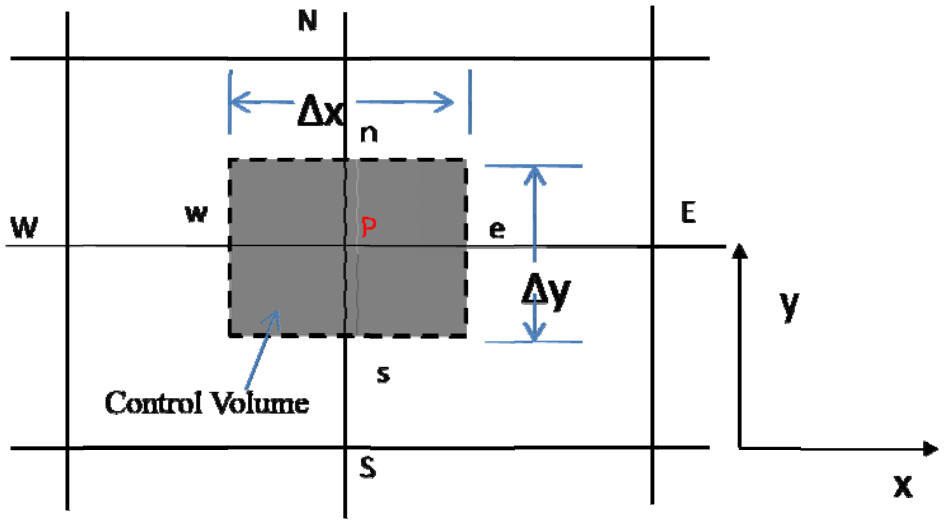

Figure 2.5 Two Dimensional Control Volume

We can calculate the heat flux q_e at the control-volume face between P and E. We shall assume that q_e, thus obtained, prevails over the entire face of area Δy x 1.Heat flow rates through the other faces can be obtained in a similar fashion. In this manner, the differential equation can be turned into the discretization equation

$$\int_t^{t+\Delta t}\int_{CV}\rho c\frac{\partial T}{\partial t}dVdt=\int_t^{t+\Delta t}\int_{CV}\frac{\partial}{\partial x}(K\frac{\partial T}{\partial x})dVdt+\int_t^{t+\Delta t}\int_{CV}\frac{\partial}{\partial x}\left(K\frac{\partial T}{\partial y}\right)+\int_t^{t+\Delta t}\int_{CV}sdVdt \tag{2.19}$$

This may be written as

$$\int_w^e\left[\int_t^{t+\Delta t}\rho c\frac{\partial T}{\partial t}dt\right]dV=\int_t^{t+\Delta t}\left[\left(KA\frac{\partial T}{\partial x}\right)_e-\left(KA\frac{\partial T}{\partial x}\right)_w\right]dt+\int_t^{t+\Delta t}\left[\left(KA\frac{\partial T}{\partial y}\right)_n-\left(KA\frac{\partial T}{\partial y}\right)_s\right]dt$$

$$+\int_t^{t+\Delta t}\bar{S}\Delta Vdt \tag{2.20}$$

In equation A is the face area of the control volume,ΔV is its volume, which is equal to AΔx where Δx is the width of the control volume in x direction and in y direction ΔV is equal to AΔy, where Δy is the width of the control volume in y direction. $\bar{S}$ is the average source

strength. If the temperature at a node is assumed to prevail over the whole control volume, the left hand side can be written as

$$\int_{CV}\left[\int_{t}^{t+\Delta t}\rho c\frac{\partial T}{\partial t}dt\right]dV=\rho c\left(T_P-T_P{}^o\right)\Delta V \tag{2.21}$$

In equation (2.21) superscript '*o*' refers to temperature at time *t*; temperatures at time level t+Δt are not superscripted. The same result as (2.21) would be obtained by substituting $\left(T_P-T_P{}^o\right)\big/\Delta t$ for $\frac{\partial T}{\partial t}$ so this term has been discretised using a first (backward) differencing scheme. If we apply central differencing schemes to the diffusion terms on the right hand side equation (2.20) may be written as

$$\rho c\left(T_P-T_P{}^o\right)\Delta V=\int_{t}^{t+\Delta t}\left[\left(K_eA_e\frac{T_E-T_P}{\delta x_{PE}}\right)-\left(K_wA_w\frac{T_P-T_W}{\delta x_{WP}}\right)\right]dt$$

$$+\int_{t}^{t+\Delta t}\left[\left(K_nA_n\frac{T_N-T_P}{\delta y_{PN}}\right)-\left(K_sA_s\frac{T_P-T_S}{\delta y_{SP}}\right)\right]dt+\int_{t}^{t+\Delta t}\overline{S}\Delta V dt \tag{2.22}$$

To evaluate the right hand side of this equation we need to make an assumption about the variation of T_P, T_E, T_W, T_N, and T_S with time. We could use temperatures at time t or at time *t*+Δ*t* to calculate the time integral or, alternatively, a combination of temperatures at time *t*+Δ*t*. We may generalize the approach by means of a weighing parameter *θ* between 0 and 1 and write the integral I_T of temperature T_P with respect to time as

$$I_T=\int_{t}^{t+\Delta t}T_Pdt=\left[\theta T_P+(1-\theta)T_P{}^o\right]\Delta t \tag{2.23}$$

Hence

θ	0	1/2	1
I_T	$T_P{}^0\Delta t$	$\frac{1}{2}\left(T_P+T_P{}^o\right)\Delta t$	$T_P\Delta t$

If *θ*=0 the temperature at (old) time level *t* is used; if *θ*=1 the temperature at new time level *t*+Δ*t* is used; and finally if *θ*=1/2, the temperature at *t* and *t*+Δ*t* are equally weighed.

Using formula for T_W and T_E and T_S and T_N in equation, and dividing by Δt throughout, we have

$$\rho c\left(\frac{T_P - T_P{}^o}{\Delta t}\right)\Delta x\Delta y = \theta\left[\frac{K_e A_e(T_E - T_P)}{\delta x_{PE}} - \frac{K_w A_w(T_P - T_W)}{\delta x_{WP}}\right]$$

$$+(1-\theta)\left[\frac{K_e A_e\left(T_E{}^o - T_P{}^o\right)}{\delta x_{PE}} - \frac{K_w A_w\left(T_P{}^o - T_W{}^o\right)}{\delta x_{WP}}\right]$$

$$+\theta\left[\frac{K_n A_n(T_N - T_P)}{\delta y_{PN}} - \frac{K_s A_s(T_P - T_S)}{\delta y_{SP}}\right]$$

$$+(1-\theta)\left[\frac{K_n A_n\left(T_N{}^o - T_P{}^o\right)}{\delta y_{PN}} - \frac{K_s A_s\left(T_P{}^o - T_S{}^o\right)}{\delta y_{SP}}\right] + \bar{S}\Delta x\Delta y \qquad (2.24)$$

This may be rearranged to give

$$\left[\rho c\frac{\Delta x\Delta y}{\Delta t} + \theta\left(\frac{K_e A_e}{\delta x_{PE}} + \frac{K_w A_w}{\delta x_{WP}} + \frac{K_n A_n}{\delta y_{PN}} + \frac{K_s A_s}{\delta y_{SP}}\right)\right]T_P = \frac{K_e A_e}{\delta x_{PE}}\left[\theta T_E + (1-\theta)T_E{}^o\right] + \frac{K_w A_w}{\delta x_{WP}}\left(\theta T_W + (1-\theta)T_W{}^o\right)$$

$$+\frac{K_n A_n}{\delta y_{PN}}\left[\theta T_N + (1-\theta)T_N{}^o\right] + \frac{K_s A_s}{\delta y_{SP}}\left[\theta T_S + (1-\theta)T_S{}^o\right]$$

$$+\left[\rho c\frac{\Delta x\Delta y}{\Delta t} - (1-\theta)\frac{K_e A_e}{\delta x_{PE}} - (1-\theta)\frac{K_w A_w}{\delta x_{WP}} - (1-\theta)\frac{K_n A_n}{\delta y_{PN}} - (1-\theta)\frac{K_s A_s}{\delta y_{SP}}\right]T_P{}^o + \bar{S}\Delta x\Delta y \qquad (2.25)$$

$$a_P T_P = a_W\left[\theta T_W + (1-\theta)T_W{}^o\right] + a_E\left[\theta T_E + (1-\theta)T_E{}^o\right] + a_S\left[\theta T_S + (1-\theta)T_S{}^o\right] + a_N\left[\theta T_N + (1-\theta)T_N{}^o\right]$$

$$+\left[a_P{}^o - (1-\theta)a_W - (1-\theta)a_E - (1-\theta)a_S - (1-\theta)a_N\right]T_P{}^o + \bar{S}\Delta x\Delta y \qquad (2.26)$$

$$a_P = a_P{}^o + \theta(a_W + a_E + a_S + a_N)$$

For implicit scheme the value of θ is 1.The equation can be written as

$$a_P T_P = a_E T_E + a_W T_W + a_N T_N + a_S T_S + b \qquad (2.27)$$

$$a_P{}^o = \rho c\frac{\Delta x\Delta y}{\Delta t}$$

$$b = S_C \Delta x \Delta y + a_P{}^o T_P{}^o$$

$$a_P = a_E + a_W + a_N + a_S + a_P{}^o - S_P \Delta x \Delta y$$

The product $\Delta x\ \Delta y$ is the control volume.

	1 *D*	2 *D*
ΔV	Δx	$\Delta x \Delta y$
$A_w = A_e$	1	Δy
$A_n = A_s$	---	Δx

	a_W	a_E	a_S	a_N
2*D*	$\frac{K_w A_w}{\delta x_{WP}}$	$\frac{K_e A_e}{\delta x_{PE}}$	$\frac{K_s A_s}{\delta y_{SP}}$	$\frac{K_n A_n}{\delta y_{PN}}$

2.6 Solutions of Algebraic Equations:

Direct Methods (i.e., those requiring no iteration) for solving the algebraic equations arising in two or three-dimensional problems are much more complicated and require rather large amounts of computer storage and time. For a linear problem, which requires the solution of the algebraic equations only once, a direct method may be acceptable; but in nonlinear problems, since the equations have to be solved repeatedly with updated coefficients, the use of a direct method usually not economical. We shall, therefore exclude direct methods from further consideration.

The alternative method then is iterative methods for the solution of algebraic equations. These start from a guessed field of *T* (the dependent variable) and use the algebraic equations in some manner to obtain an improved field. Successive repetitions of the algorithm finally lead to a solution that is sufficiently close to the correct solution of the algebraic equations. Iterative methods usually require very small additional storage in the

computer, because only non-zero coefficients of the equations are stored in core memory. So they are especially useful for handling nonlinearities.

There are many iterative methods for solving algebraic equations. Some of the examples are the Jacobi and Gauss-Seidel point-by-point iteration methods.

Jacobi and Gauss-Seidel iterative methods are easy to implement in simple computer programs, but they can be slow to converge when the system of equations is large. Hence they are not considered suitable for rapidly solving tri-diagonal systems that is now called Thomas algorithm or the tri-diagonal matrix algorithm (TDMA). The TDMA is actually a direct method for one-dimensional situations, but it can be applied iteratively, in a line-by-line fashion, to solve multi-dimensional problems. It is computationally inexpensive and has the advantage that it requires a minimum amount of storage.

2.6.1 The Tri-diagonal Matrix Algorithm:

TDMA refers to the fact that when the matrix of the coefficients of these equations is written, all the nonzero coefficients align themselves along three diagonals of the matrix.

Suppose the grid points were numbered 1, 2, 3, ……, N , with points 1 and N denoting the boundary points. The discretization equations can be written as

$$a_i T_i = b_i T_{i+1} + c_i T_{i-1} + d_i \tag{2.28}$$

for i=1, 2, 3, ……..,N. Thus the temperature T_i is related to the neighboring temperatures T_{i+1} and T_{i-1}. To account for the special form of the boundary-point equations, let us set

$$c_1=0 \quad \text{and} \quad b_N=0,$$

so that the temperatures T_0 and T_{N+1} will not have any meaningful role to play. (When the boundary temperatures are given, these boundary-point equations take a rather trivial form. For example, if T_1 is given, we have a_1=1, b_1=0, c_1=0, and d_1=the given value of T_1.)

These conditions imply that T_1 is known in terms of T_2. The equation for i=2 is a relation between T_1, T_2, and T_3. But, since T_1 can be expressed in terms of T_2, this relation reduces to a relation between T_2 andT_3. In other words, T_2 can be expressed in terms of T_3. This process of substitution can be continued until T_N is formally expressed in terms of T_{N+1}. But, because T_{N+1} have no meaningful existence, we actually obtain the numerical value of T_N at this stage. This enables us to begin the "back-substitution" process in which T_{N-1} is

obtained from T_N, T_{N-2} from T_{N-1},……,T_2 from $T3$, and T_1 from T_2. This is the essence of TDMA. Suppose in the forward- substitution process, we seek a relation

$$T_i=P_iT_{i+1}+Q_i \tag{2.29}$$

Similarly we can also write

$$T_{i-1}= P_{i-1}T_i +Q_{i-1} \tag{2.30}$$

Substitution of equation (2.30) into equation (2.28) leads to

$$a_iT_i=b_iT_{i+1}+c_i(P_{i-1}T_i+Q_{i-1}) + d_i \tag{2.31}$$

The coefficients P_i and Q_i are

$$P_i = \frac{b_i}{a_i - c_iP_{i-1}},$$

$$Q_i = \frac{d_i + c_iQ_{i-1}}{a_i - c_iP_{i-1}}$$

These are the recurrence relations, since they give P_i and Q_i in terms of P_{i-1} and Q_{i-1}. To start the Recurrence process, we note that equation (2.28) for i=1 is almost of the form (2.30). Thus the values of P_1 Q_1 are given by

$$P_1 = \frac{b_1}{a_1}$$

$$Q_1 = \frac{d_1}{a_1}$$

Discussion: (1) The discretization equations for the grid points along a chosen line are considered. They contain the temperature at the grid points along the neighboring lines. If these temperatures are substituted from their latest values, the equation for the grid points along the chosen line would look like one-dimensional equations and could be solved by the TDMA. This procedure is carried out for all the lines in the y-direction and may be followed by a similar treatment for the x-direction.

(2) The convergence of the line-by-line method is faster, because the boundary-condition information from the ends of the line is transmitted at once to the interior of the domain, no matter how many grid points lie in one line.

2.7 Computational Domain:

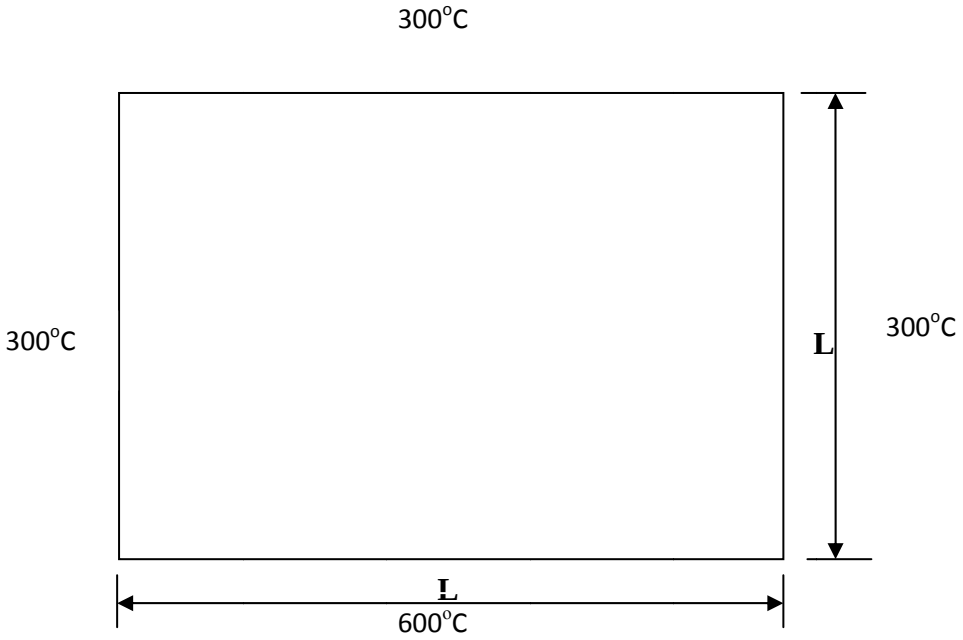

Figure 2.6 Computational Domain

2.8 Flow Chart For Solving Transient Conduction:

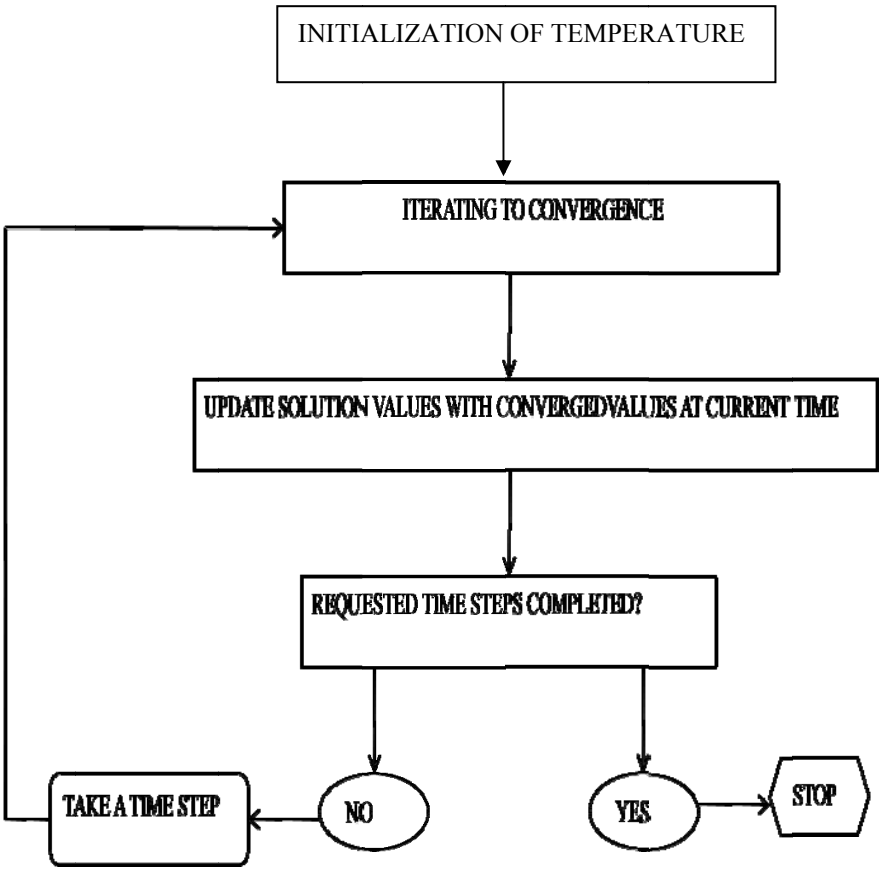

CHAPTER 3

RADIATIVE HEAT TRANSFER

3. RADIATIVE HEAT TRANSFER:

3.1 Mathematical Description of Radiation:

We refer as radiative energy transfer to the variation of the energy of any system due to absorption or emission of electromagnetic waves. From a physical point of view, such electromagnetic waves can be understood as a group of mass less particles that propagate at the speed of light '*c*'. Each of these particles carries an amount of energy, inversely proportional to the wavelength of its associated wave. Such particles are photons. A single photon represents a plane wave; therefore we are forced to assume that it propagates along a straight path. Because of this, we can think of a system loosing energy by emitting a number of photons, or gaining energy by absorbing them.

Radiation heat transfer presents a number of unique characteristics. First of all, the amount of radiative heat transfer does not depend on linear differences of temperature, but on the difference of the fourth power of the temperature. This fact implies that, at high temperatures, radiative energy transfer should be taken into account, particularly if large differences in temperature exist. Furthermore, it is the only one form of energy transfer in vacuum. Therefore, in vacuum applications, radiation should be taken into account, even low temperatures. And, of course, it should be taken into account for study of devices which use solar energy.

On the other hand, radiation can be neglected if there are no significant temperature differences in a given system, and also if highly reflective walls are present.

As the photons propagate along straight paths, we also need to know, at every spatial location, the number of photons propagating in a given solid angle. Under the assumption of straight propagation, we are neglecting the wave properties of radiation.

The photon density is defined as the number of photons, with wavelength between λ and $\lambda + d\lambda$, crossing an area dA perpendicular to the photon direction $\hat{s}$ within a solid angle $d\Omega$, per unit time dt and per unit wavelength $d\lambda$. It is more useful to consider the energy density I instead of the photon density. The energy density is simply the number of photons multiplied by the energy of each photon. The energy density is usually named intensity radiation field, and its physical meaning is therefore

$$I(r,\hat{s},\lambda) = \frac{Energy\ of\ wavelength\ \lambda\ through\ an\ area\ normal\ to\ \hat{s}}{dAd\Omega d\lambda dt} \tag{3.1}$$

From this definition is clear that, for a fixed point and wavelength, the intensity radiation field is a function defined over the unit sphere, and therefore is not a conventional scalar field, such as the temperature. With the definition of the intensity radiation field on mind, the total energy that crosses a surface perpendicular to a given unit vector $\hat{n}$, per unit time and area, is readily obtained as

$$q(r,\bar{n}) = \int_0^\infty d\lambda \int_{4\pi} d\Omega(\hat{n}.\hat{s}) I(r,\hat{s},\lambda) \tag{3.2}$$

Where $\left(\hat{n}.\hat{s}\right)$ factor appears since *I* is defined as energy through the propagation direction $\hat{s}$.

3.2 Radiative Properties of Materials:

3.2.1 Black body radiation:

Once the mathematical tools for the description of radiation energy are settled, it would be interesting to know how much energy emits a body under different physical conditions. This one turns out to be a complicated problem, so some simplifying hypothesis is required. The simplest possible case is that of the black body.

The black body plays the same role as the ideal gas, in the sense that its behavior is the same no matter of what is made. It also serves as a basis for more complicated bodies. By definition, any body which absorbs the totality of photons is called a black body. For such a body in thermal equilibrium with its surroundings, it has to emit as much radiation energy as it absorbs, otherwise it will heat up or cool down. This fact is called the Kirchhoff law. The energy emitted by a black body depends only on its temperature, and the distribution over all wavelengths is

$$I_b(T,\lambda) = \frac{2hc^2}{\lambda^5} \frac{1}{\exp(hc/\lambda\sigma T) - 1}, \tag{3.3}$$

Where *h* is the Planck's constant, σ is the Boltzmann constant, and *c* is the speed of light. The photon emission by a black body is isotropic, that is, it does not depend on any particular direction $\hat{s}$. Therefore, by using equation (3.2), carrying out the angular integration over an hemisphere, we find that the energy emitted by a black body per unit area, time and wavelength is simply $E_b(T,\lambda) = \pi I_b(T,\lambda)$.

An important feature of a black body is the emissive power per unit area, which is readily found by integrating equation (3.3) over all wavelengths. The result is the well known Stefan-Boltzmann law, which relates the emissive power to the temperature of the black body:

$$I_b(T) = \frac{\sigma_B T^4}{\pi} \tag{3.4}$$

3.2.2 Surface properties:

Each surface will radiate a certain amount of energy due to its temperature. Such emitted energy, which will depend on the properties of the surface, its temperature, the radiation wavelength, the direction of emission leads to the definition of the emissivity of a surface. As stated before, we can use the black body as a reference to define the surface properties of real bodies. Therefore, if the surface is at temperature *T*, the emissivity is defined as

$$\varepsilon = \frac{I_{emitted}(T, \lambda, \hat{s})}{I_b(T, \lambda)} \tag{3.5}$$

As the black body is defined as the perfect radiation absorber, by the Kirchhoff law, there is no body capable of emitting more radiation energy than a black body for any given temperature. Therefore, the emissivity ε will be between zero and one.

On the other hand, when an electromagnetic wave strikes a surface, the interaction between this incident wave and the elements of the surface result on a fraction of the energy of the wave being reflected, while the remaining fraction will be absorbed (or transmitted) within the material. These fractions may very well depend on the incident angle and the wavelength of the original wave. Specifically, we can define

$$\rho = \frac{I_{reflected}}{I_{incoming}}; \ \alpha = \frac{I_{absorbed}}{I_{incoming}}; \ \tau = \frac{I_{transmitted}}{I_{incoming}}$$

The coefficients ρ, α, and τ, are the reflectivity, absorptivity, and transmissivity of the surface respectively. As the wave is either reflected, or absorbed, or transmitted, it is clear that we must have $\rho + \alpha + \tau = 1$ if the energy is to be conserved.

An important feature of reflection should be pointed out: while the reflected wave has the same angle (with respect to the normal of the surface) of the incident wave for perfectly smooth surfaces, if the surface is not polished, the angle of the reflected wave could have any value, due to multiple reflections. There is a fraction of the incoming intensity that is equally distributed for all possible outgoing directions. Due to this, the reflectivity ρ is usually

divided in a diffuse componentρ_d, and a specular component ρ_s. Therefore, a fraction ρ_d of the incoming energy will be reflected equally over all the angles, and a fractionρ_s will be reflected in an angle equal to that of the incident wave. We have of course $\rho = \rho_d + \rho_s$.

Moreover, a surface that absorbs a fraction α of the incident energy will emit the same amount of energy if it is at thermal equilibrium (the Kirchhoff law again). Therefore, we could assume that $\alpha(T, \lambda, \hat{s}) = \varepsilon(T, \lambda, \hat{s})$.

3.3 FORMULATION OF RADIATIVE TRANSFER EQUATION BY USING FV METHOD:

We are assuming that photons propagate along straight lines, hence the most natural way to examine the effect exerted by the medium on the number of photons (or equivalently on the intensity radiation field) is to analyze the intensity radiation field precisely along a straight line. In the most general case, the intensity along the direction defined by the unit vector $\hat{s}$ will depend both on the distance s in this direction, and on time t. Therefore we could write the variation of intensity with respect to s and t as

$$dI = I(s + ds, t + dt) - I(s, t) = \frac{\partial I}{\partial s} ds + \frac{\partial I}{\partial t} dt \tag{3.6}$$

Recalling that photons travel at the speed of light c, we have $ds = cdt$, and the resulting variation of intensity per unit length along the direction $\hat{s}$ is

$$\frac{dI}{ds} = \frac{\partial I}{\partial s} + \frac{1}{c}\frac{\partial I}{\partial t} \tag{3.7}$$

The speed of light is very high, resulting on the fact that, for practical purposes, we can think that the intensity radiation field instantly reacts to any changes of the physical conditions that determine it. Therefore, the partial derivative of I with respect to time t in equation, will be ignored hereinafter.

As an electromagnetic wave propagates inside a medium, it loses energy as the charged particles within the medium accelerate in response to the wave. These particles, in turn, release part of its energy in form of electromagnetic waves. In the photon framework, we think of the same process as photons being absorbed and emitted by the medium. However, if the final state of the interacting particle is the same as the initial state, we understand that the corresponding photon is simply redirected (and therefore has the same energy). We say that

such a photon is scattered. It turns out that scattered photons complicate the formulation of the radiative transfer equation (RTE), by turning a simple linear differential equation to an integro-differential one, combining differentiation with respect one set of variables (spatial location) and integration over another set of variables (solid angle).

The RTE accounts for the variation of the intensity radiation field, readily related to the number of photons, on a direction given by the unit vector $\hat{s}$. Such variation can be attributed to different phenomena, and is usually divided in three additive terms. It is written as

$$\frac{dI(r,\hat{s})}{ds} = -\beta(r)I(r,\hat{s}) + \kappa(r)I_b(r,\hat{s}) + \frac{\sigma(r)}{4\pi}\int_{4\pi} I(r,\hat{s}')\phi(\hat{s}',\hat{s})d\Omega' \tag{3.8}$$

The above equation is valid for a single wavelength. If the absorption and scattering coefficients κ and σ_s are zero, the RTE is simplified enormously. Under such conditions, we talk of a transparent medium, and for very small domains, compared to $1/\kappa$ or $1/\sigma_s$, this approximation is reliable.

The first term, which is negative, accounts for the decrease of the number of photons on the given direction, either because it is absorbed by the medium (with an absorption coefficient κ) or because it is scattered onto another direction (with a scattering coefficient σ_s). The second term has positive sign, therefore implying an increase of the number of photons. This term is due to thermal emission of photons. It is zero only if the temperature is zero, or the absorption coefficient is zero. Notice that the proportionality coefficient is the same absorption coefficient appearing in the first term. This holds under the assumption of local thermodynamic equilibrium.

The third term contributes only if the medium scatters radiation. We should take into account that any photon, propagating along a direction given by $\hat{s}'$, may be redirected to the analyzed direction $\hat{s}$. We define the function $\phi(\hat{s}',\hat{s})$ to be 4π times the probability of such redirection occurring. Then we integrate to consider all possible directions $\hat{s}'$. The function $\phi(\hat{s}',\hat{s})$ is known as the phase function. It has to be normalized, in a way that

$$\int_{4\pi} \phi(\hat{s}',\hat{s})d\Omega' = 4\pi \tag{3.9}$$

This equation merely states that the incoming photon should be scattered into some other direction. Where the extinction coefficient and source function are

$$\beta(r) = \kappa(r) + \sigma(r) \tag{3.10}$$

$$S(r,\hat{s}) = \kappa(r)I_b(r,\hat{s}) + \frac{\sigma(r)}{4\pi}\int_{4\pi} I(r,\hat{s})\Phi(\hat{s}',\hat{s})d\Omega \tag{3.11}$$

r is the position vector and $\hat{s}$ is the unit vector describing the radiation direction. Equation (3.8) indicates the intensity depends on spatial position and angular direction. To discretize it finite volume method is used. The control angle used here are the solid angle proposed and used by Raithbay and coworkers[27-29]. Following the control volume spatial discretization practice, the angular space is subdivided into N_θ X N_ϕ =M control angles in any desired manner.

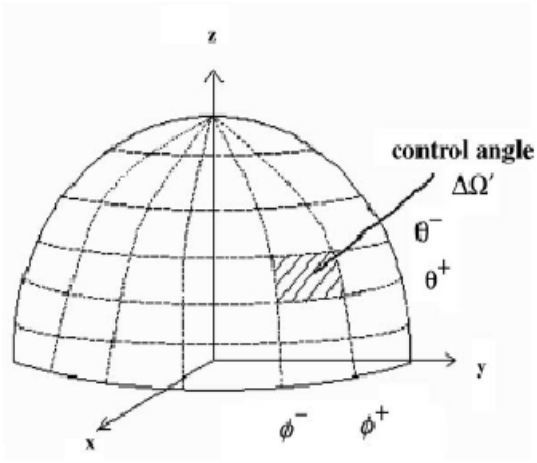

Figure 3.1Typical control angle

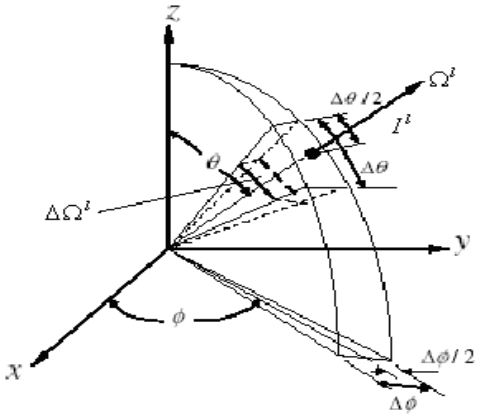

Figure 3.2 Intensity I^l in direction $\Delta\Omega^l$ in the center of the elemental sub-solid angle Ω^l

Integrating equation (3.8) over a typical two-dimensional Δv and $\Delta\Omega^l$ gives

$$\int_{\Delta\Omega'}\int_{\Delta v}\frac{dI'}{ds}dvd\ \Omega' = \int_{\Delta\Omega'}\int_{\Delta v}(-\beta I^l + S^l)\,dvd\ \Omega^l \tag{3.12}$$

where

$I' \equiv I(r,\hat{s}')$.

Applying the divergence theorem, Eq(3.12) becomes

$$\int_{\Delta\Omega^l}\int_{\Delta A} I^l(\hat{s}^l.\hat{n})dAd\Omega^l = \int_{\Delta\Omega^l}\int_{\Delta v}(-\beta I^l + S^l)dvd\Omega^l \tag{3.13}$$

The left side of the equation represents the inflow and outflow of radiant energy across the four control volume faces. The right hand side denoted the attenuation and augmentation of energy within a control volume. Following the practice of control volume approach, the intensity is assumed constant within a control volume and a control angle. So Eq.(3.13) can be simplified to

$$\sum_{i=1}^{4} I^l{}_i\Delta A_i \int_{\Delta\Omega^l}(\hat{s}^l.\hat{n}_i)d\Omega^l = (-\beta I^l + S^l)\Delta v\Delta\Omega' \tag{3.14}$$

Where

$$S' = \kappa I_b + \frac{\sigma_s}{4\pi}\sum_{r=1}^{M} I^{l'}\overline{\Phi}^{l'l}\Delta\Omega^{l'} \tag{3.15}$$

In Eq. (3.15), the radiation direction varies within a control angle, whereas the magnitude of the intensity is assumed constant. If the radiation direction is fixed at a given direction within a control angle and the magnitude of intensity is constant, the discretization equation for the discrete ordinates method [30] is obtained.

Following the treatment presented by chai et al;[30] a modified extinction coefficients and a modified source function can be written for a discrete direction l as

$$\beta_m^l = \beta - \frac{\sigma_s}{4\pi}\overline{\Phi}^{l'l}\Delta\Omega^{l}$$

$$S_m^l = \kappa I_b + \frac{\sigma_s}{4\pi}\sum_{l'=1,l'\neq l}^{M} I^{l'}\overline{\Phi}^{l'l}\Delta\Omega^{l'}$$

With this modification, Eq. (3.14) becomes

$$\sum_{i=1}^{4} I^{l}{}_{i}\Delta A_i \int_{\Delta\Omega^l}(\hat{s}^l.\hat{n}_i)d\Omega^l = (-\beta'_m I^l + S'_m)\Delta v\Delta\Omega' \tag{3.16}$$

For the typical control volume and radiation direction shown in Fig, Eq.(3.16) can be further simplified to

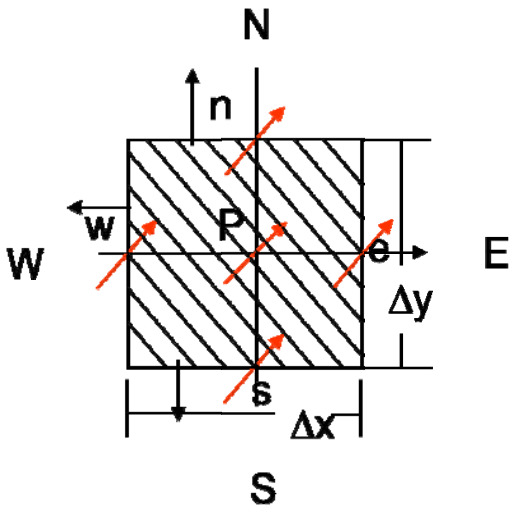

Figure 3.3 Control angle orientations

$$(I_e^{\ l} - I_w^{\ l})\Delta A_x D_{cx}^{\ l} + (I_n^{\ l} - I_s^{\ l})\Delta A_y D_{cy}^{\ l} = [-(\beta_m^{\ l})_p I^l{}_p + (S_m^{\ l})_p]\Delta v\Delta\Omega^l \tag{3.17}$$

To relate the boundary intensities to the nodal intensity, spatial differencing schemes are needed. One available scheme is the step scheme which sets the downstream boundary intensities equal to the upstream nodal intensities;

$$I_P^l = I_e^l = I_n^l, I_s^l = I_S^l, I_w^l = I_W^l$$

From the above fig, the step scheme discretization equation can be written as

$$a_p^l I_p^l = a_W^l I_W^l + a_S^l I_S^l + b \tag{3.18}$$

$$a_W^l = \Delta y D_{cx}^l$$
$$a_S^l = \Delta x D_{cy}^l$$
$$a_p^l = \left[\Delta x D_{cy}^l + \Delta y D_{cx}^l + (\beta_m^l)_p \Delta v \Delta\Omega^l\right]$$

Where

$$b' = (S_m^l)_p \Delta v \Delta\Omega^l$$

$$\Delta\Omega' = \int_{\phi_1}^{\phi_2}\int_{\theta_1}^{\theta_2} \sin\theta \, d\theta \, d\Phi \tag{3.19}$$

$$D_{cex}^l = \int (\hat{s}^l . \hat{n}_x) d\Omega^l = \int_{\phi_1}^{\phi_2}\int_{\theta_1}^{\theta_2} \sin\theta\cos\phi\sin\theta d\theta d\phi = -D_{cwx}^l = D_{cx}^l \tag{3.20}$$

$$D_{cny}^l = \int (\hat{s}^l . \hat{n}_y) d\Omega^l = \int_{\phi_1}^{\phi_2}\int_{\theta_1}^{\theta_2} \sin\theta\sin\phi\sin\theta d\theta d\phi = -D_{csy}^l = D_{cy}^l \tag{3.21}$$

3.4 SOLUTION PROCEDURE:

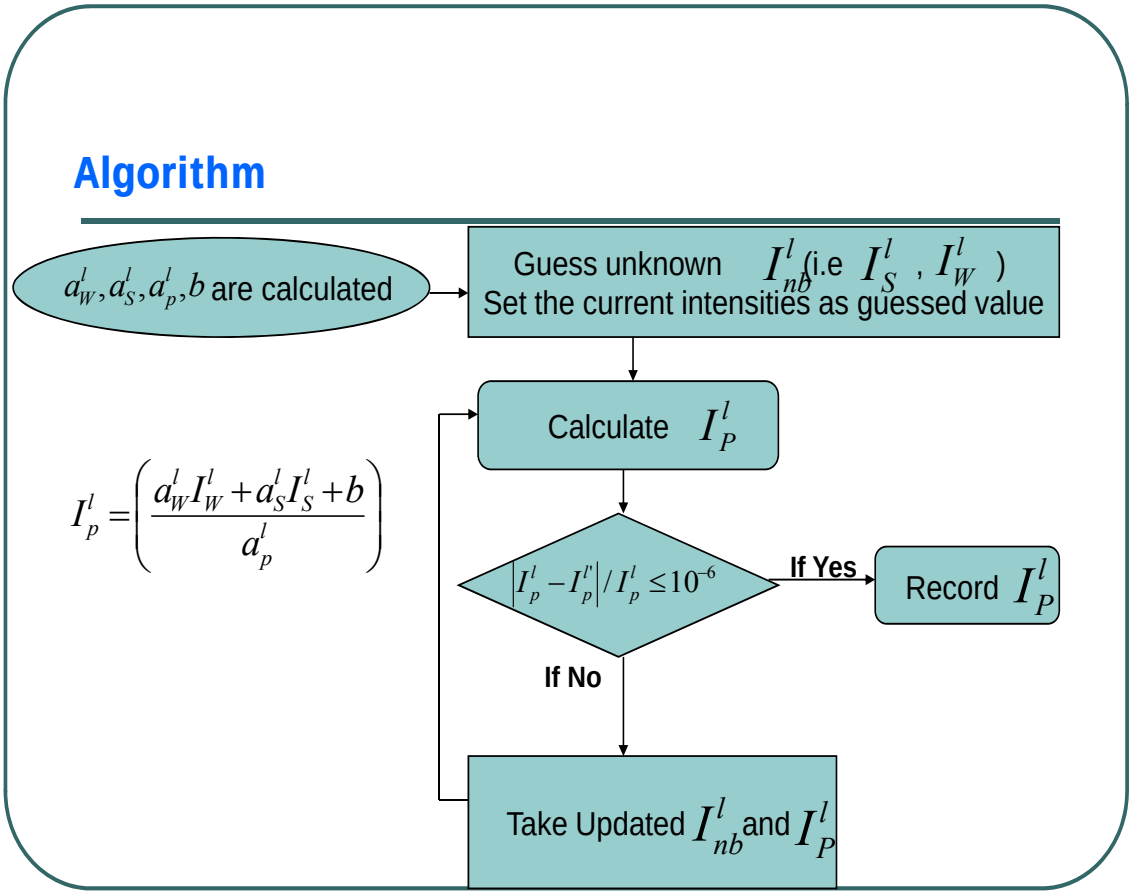

Figure 3.4 Flowchart for overall solution procedure

CHAPTER 4

ANALYSIS

4. ANALYSIS

4.1 ENERGY EQUATION

The transient state energy conservation equation consisting of both conduction and radiation in an infinitesimal control volume can be expressed as

$$\rho c \frac{\partial T}{\partial t} = K\nabla^2 T - \nabla . q_R \tag{4.1}$$

It is assumed that the thermal conductivity K of the medium is independent of temperature T of the medium. The divergence of the radiative heat flux is given by

$$\nabla . q_R = \kappa(4\pi I_b - G) \tag{4.2}$$

Where κ is the absorption coefficient, I_b is the blackbody intensity and G is the incident radiation. Substituting Eq.(4.2) into Eq(4.1), the non dimensional equation can be expressed as

$$\frac{\partial \theta}{\partial \xi} = \frac{1}{L^2\beta^2}\frac{\partial^2 \theta}{\partial X^2} + \frac{1}{H^2\beta^2}\frac{\partial^2 \theta}{\partial Y^2} - \frac{(1-\omega)}{N}\left[\theta^4 - \frac{G^*}{4\pi}\right] \tag{4.3}$$

$$\theta = \frac{T}{T_{ref}},\ N = \frac{K\beta}{4\sigma T_{ref}{}^3},\ G^* = \frac{G}{\sigma T_{ref}{}^4/\pi}$$

Here in the above equation, T_{ref} is the reference temperature, σ is the Stefan-Boltzmann constant, N is the conduction radiation parameter and β is the extinction coefficient of the medium.

4.2 Calculation of incident radiation and heat flux

For calculation of the divergence of radiative heat flux, incident radiation G distribution is required. It can be calculated as

$$G(\vec{r}) = \int_{4\pi} I(\vec{r}, \hat{s}) d\Omega$$

$$= \int_{\phi=0}^{2\pi}\int_{\theta=0}^{\pi} I \sin\theta d\theta d\phi \tag{4.5}$$

The radiative heat flux in *x*, *y* and *z* directions can be calculated as

$$q_{R,x}(\vec{r}) = \int_{4\pi} I(\vec{r},\hat{s})(\hat{s}.\hat{e}_x)d\Omega$$

$$= \int_{\phi=0}^{2\pi}\int_{\theta}^{\pi} I \sin\theta\cos\phi\sin\theta d\theta d\phi \tag{4.6}$$

$$q_{R,y}(\vec{r}) = \int_{4\pi} I(\vec{r},\hat{s})(\hat{s}.\hat{e}_y)d\Omega$$

$$= \int_{\phi=0}^{2\pi}\int_{\theta}^{\pi} I \sin\theta\sin\phi\sin\theta d\theta d\phi \tag{4.7}$$

$$q_{R,z}(\vec{r}) = \int_{4\pi} I(\vec{r},\hat{s})(\hat{s}.\hat{e}_z)d\Omega$$

$$= \int_{\phi=0}^{2\pi}\int_{\theta}^{\pi} I \cos\theta\sin\theta d\theta d\phi \tag{4.8}$$

The total heat flux q_T is the summation of both conductive and radiative heat fluxes. In non-dimensional form, total heat flux in any direction(e.g. *x* direction can be expressed as)

$$\frac{q_{T,x}}{\sigma T_{ref}^{\ 4}} = -4N\frac{\partial\theta}{\partial\tau_X} + \frac{q_{R,x}}{\sigma T_{ref}^{\ 4}} \tag{4.9}$$

Where τ_x ($=\beta x$) is the optical thickness of the medium in *x*-direction

CHAPTER 5

RESULTS AND DISCUSSION

In this section, the results obtained by solving the governing equation meant for coupled conduction and radiation phenomena within an enclosure, have been delineated **.**In order to sense the effect of radiative properties of the medium and surface emissivity, at first, pure conduction phenomena has been discussed. The transient effect has also been discussed. In the figure 5.1 the temperature distribution for steady state conduction for the computational domain has been shown. The symmetry about X=0.5, is observed as expected. The heat flux variations at bottom wall, top wall and side wall are shown in the fig. 5.2, fig.5.3, fig. 5.4, the hot (bottom) wall compared to the portions nearing side walls. Where as the phenomenon is

reversed at the top cold wall. Heat flux at the bottom portion of the side walls is found to be intensive in nature respectively. It is observed that less amount of heat gets transferred at the central portion of the bottom wall.

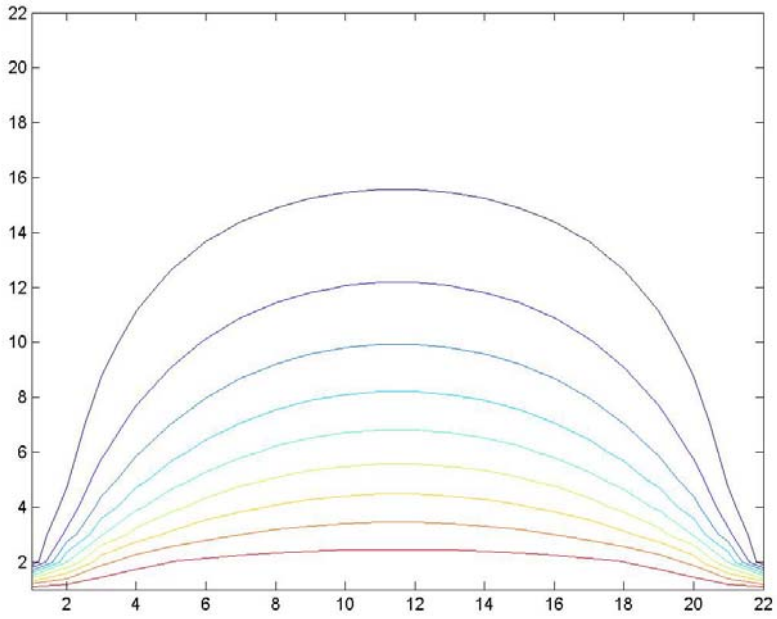

Figure 5.1 Temperature isotherms at the steady state.

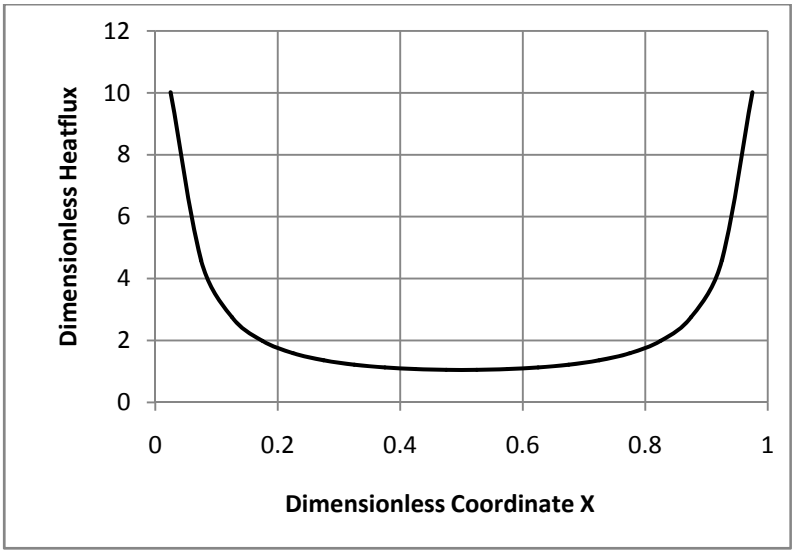

Figure 5.2 Variation of Heat flux at the bottom wall along X-axis

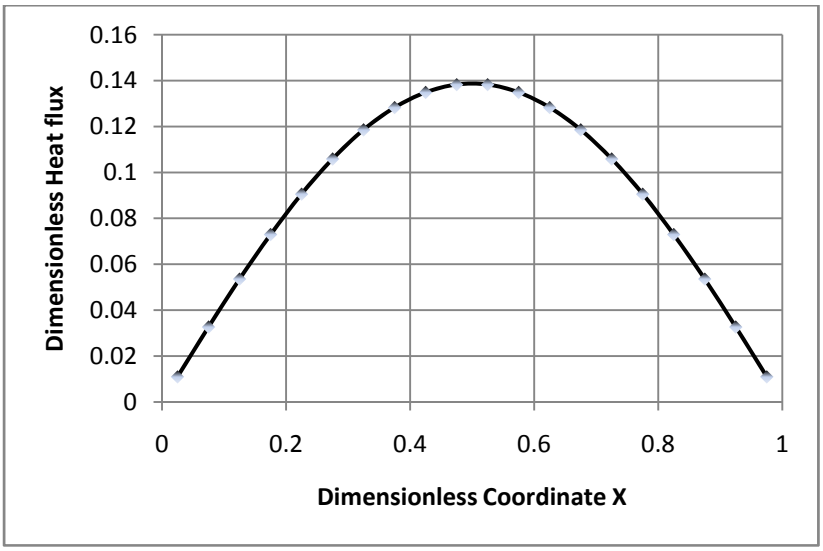

Figure 5.3 Variation of heat flux at the top cold wall with X axis

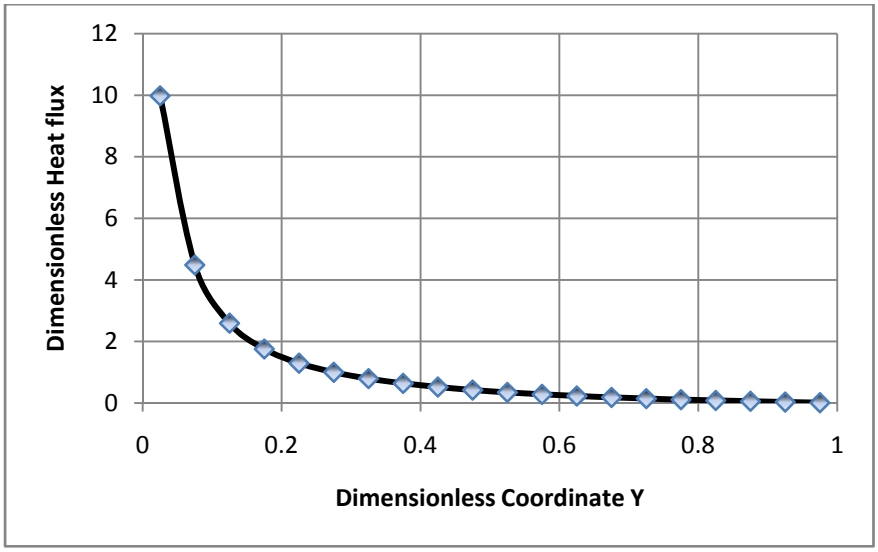

Figure 5.4 Variation of heat flux at the side cold wall with Y-axis

Before illustrating the effect of radiative properties of the participating medium on combined conduction and radiation phenomena, the validation of the present code has been made against the work Kim and Baek[17] (shown in the figure).

Figures shows the temperature along the y-direction at the symmetry line X=0.5 for various values of N. In addition ω=0 is assumed, which represents a non-scattering medium in which the radiation is emitted and absorbed only. As N decreases, radiation plays a more significant role than conduction. Therefore as N decreases, a steeper temperature gradient is formed at both top and bottom walls and the medium temperature inside increases.

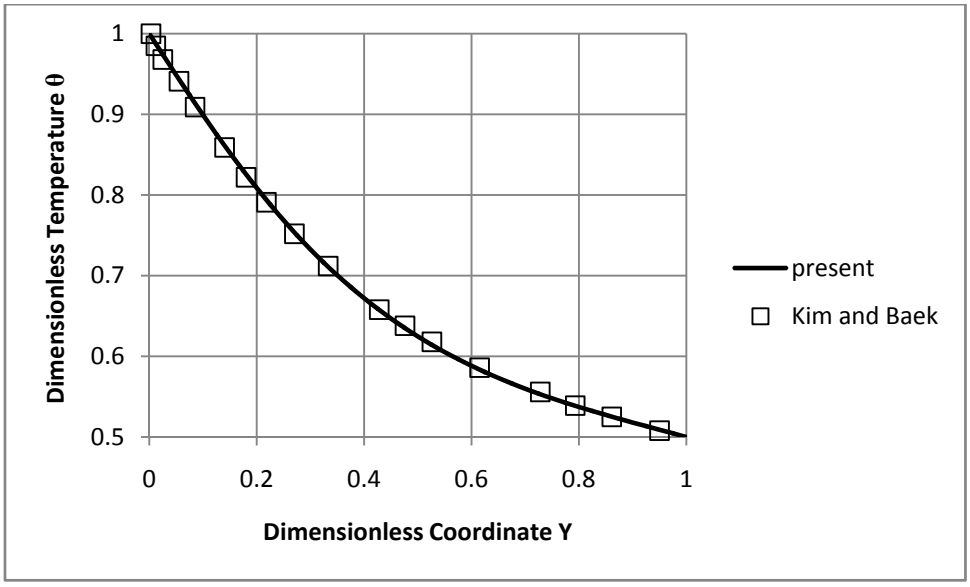

Figure 5.5 Dimensionless temperature profiles for N=1

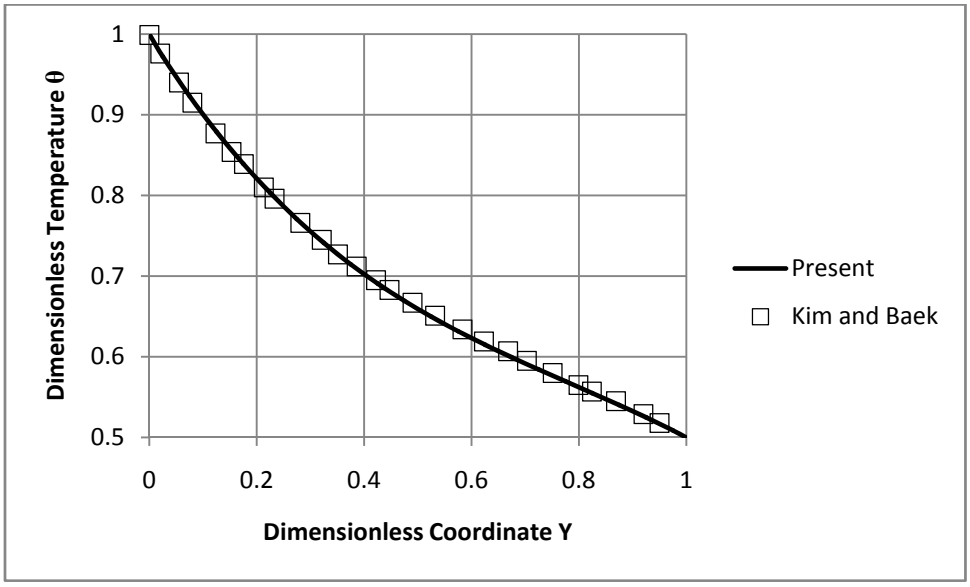

Figure 5.6 Dimensionless temperature profiles for N=0.1

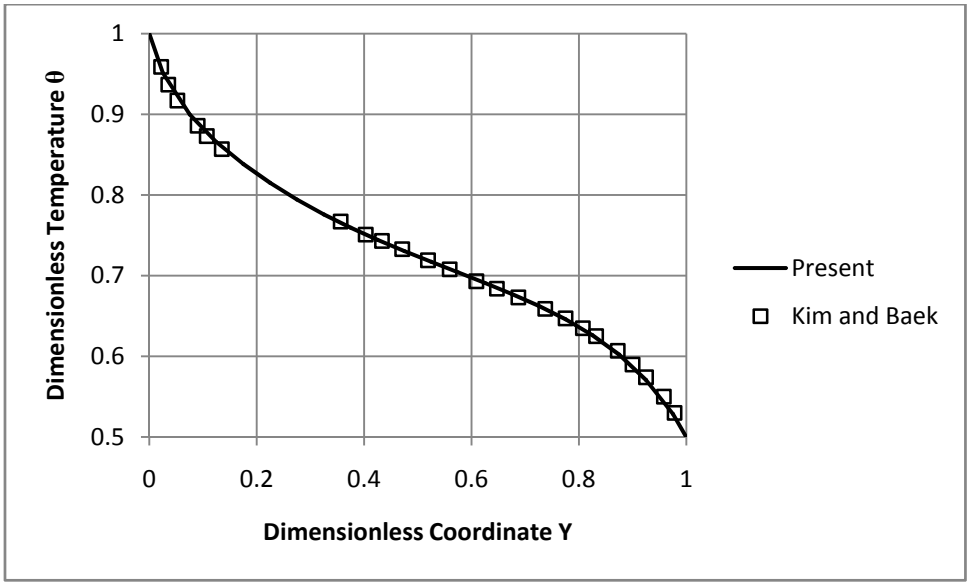

Figure 5.7 Dimensionless temperature profiles for N=0.01

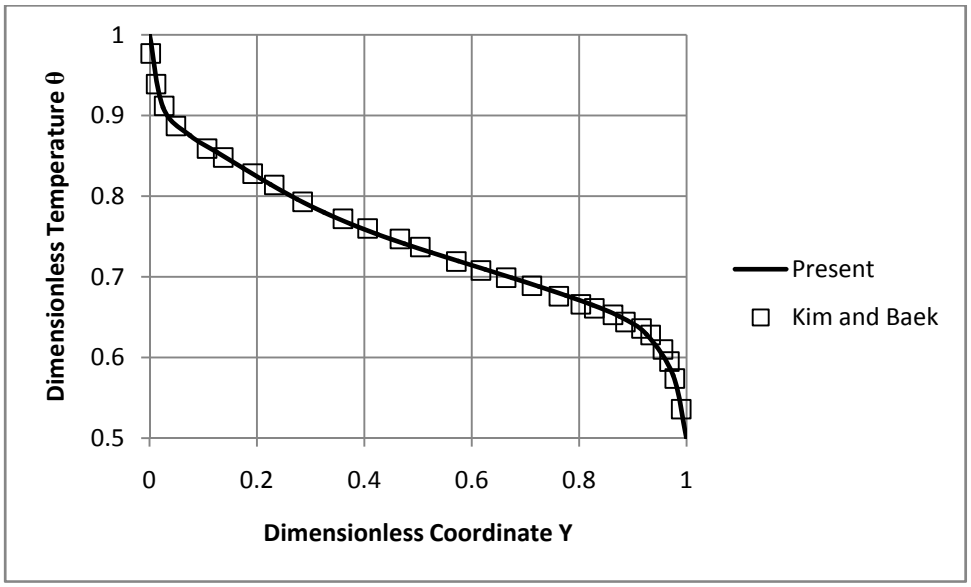

Figure 5.8 Dimensionless temperature profiles for N=0.001

5.3 Effect of Conduction- radiation parameter (N)

In general the fractional radiative heat flux is seen to decrease as N increases. In the hot wall corner region, extremely large temperature gradient produces a great deal of conductive heat flux as N increases. For N=0.001, Q^R/Q becomes nearly uniform along both end walls as shown in the figure. In this study conduction radiation parameter N is varying, keeping ε_w =1, and τ_l=1. Figure shows how fractional radiative heat flux changes with different values of conduction radiation parameter in bottom hot wall and cold top wall.

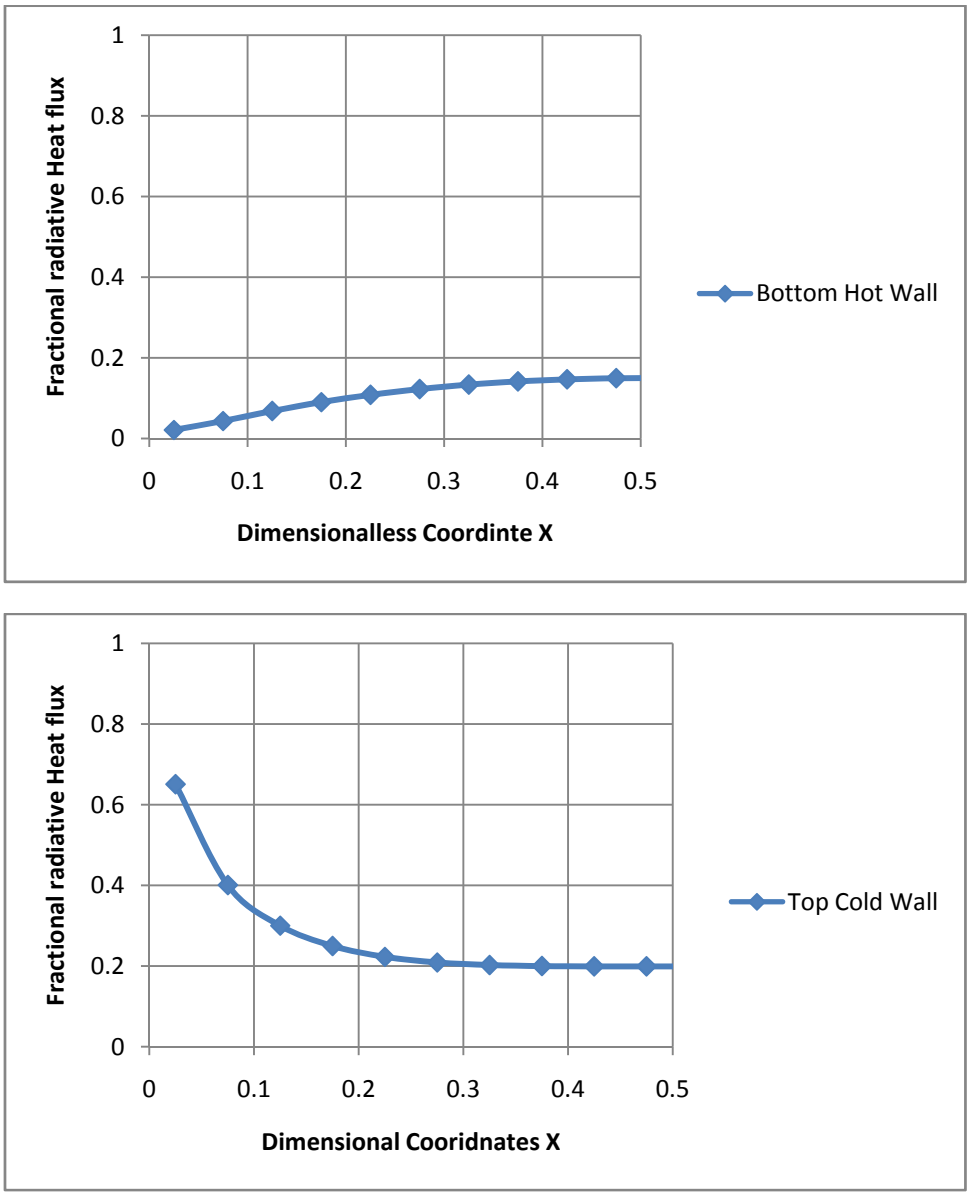

Figure 5.9 Variation of fractional radiative heat flux for N=1;

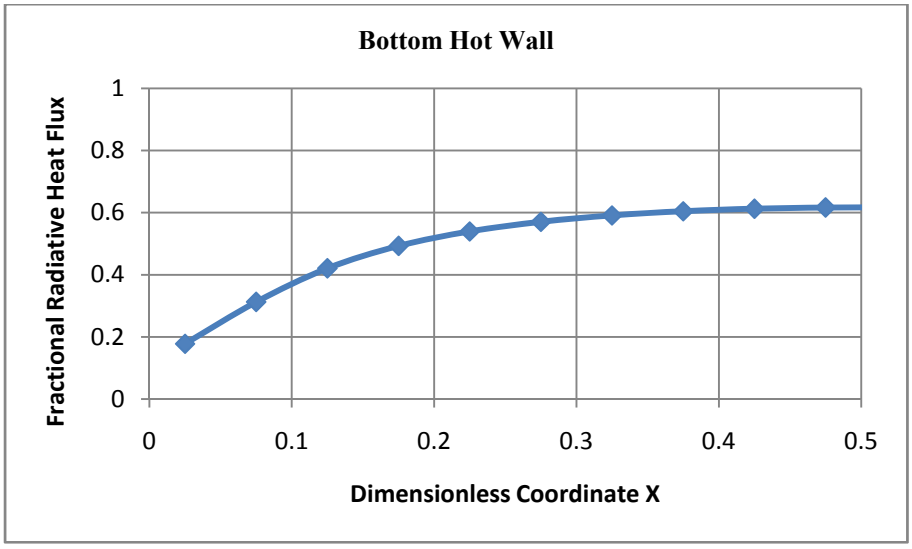

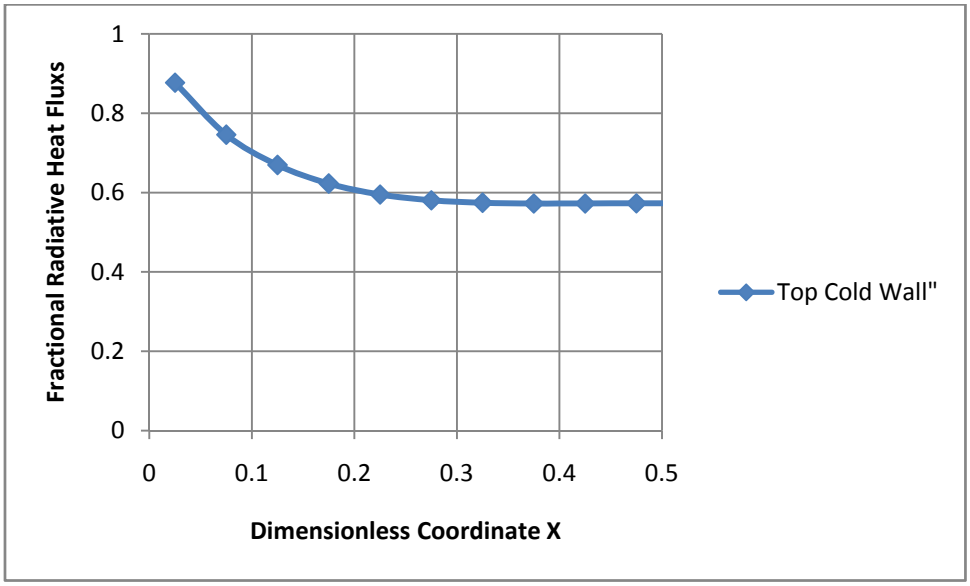

Figure 5.10 Variation of fractional radiative heat flux for N=0.1;

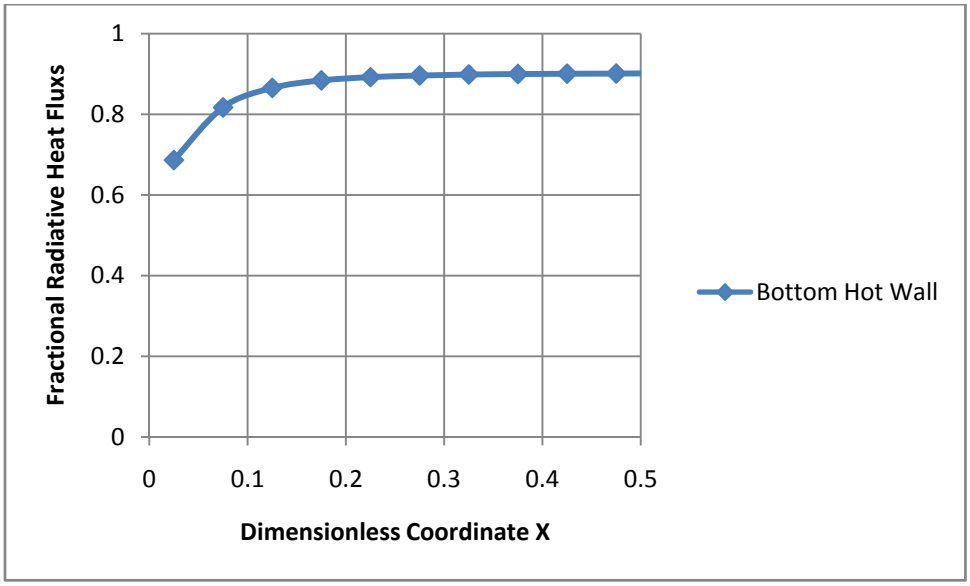

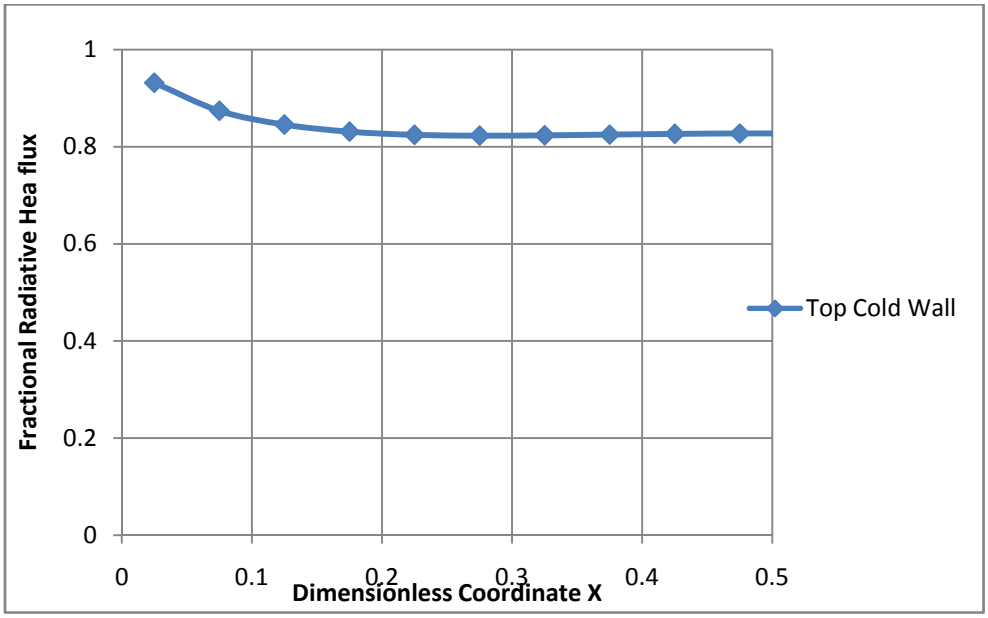

Figure 5.11 Variation of fractional radiative heat flux for N=0.01;

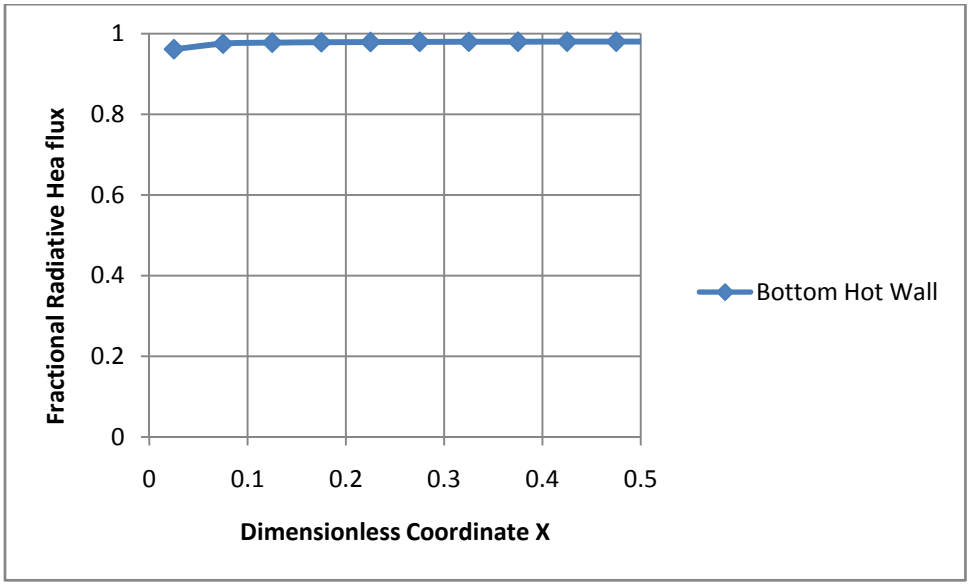

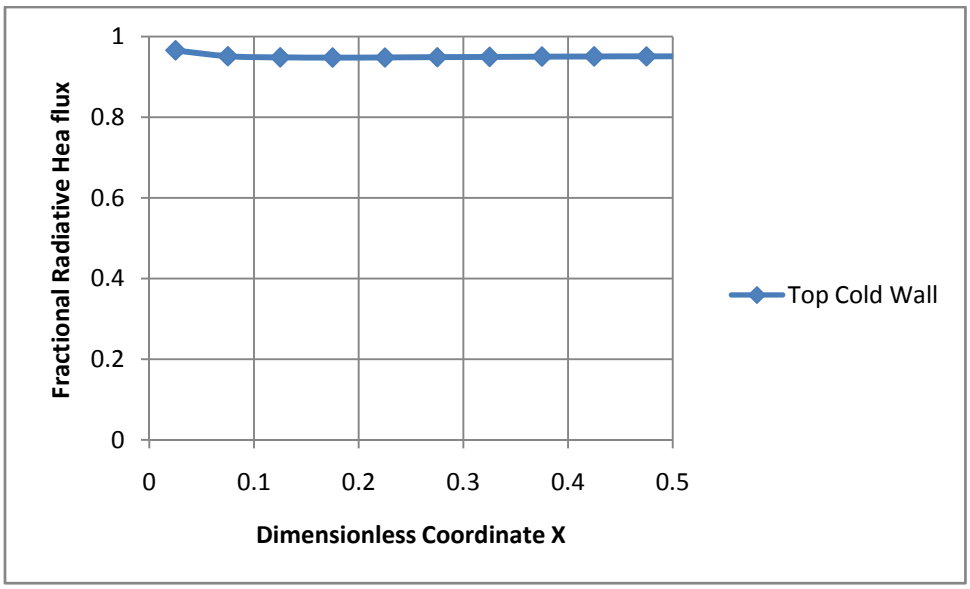

Figure 5.12 Variation of fractional radiative heat flux for N=0.001;

5.4 Effect of wall emissivities at the hot bottom wall, keeping N=0.05, τ_l=1and ω=0.

As the wall emissivity increases, the intensity at the hot wall becomes strong and it further increases the radiative heat flux and the temperature of the medium inside. The temperature gradient in the vicinity of the hot wall is thus reduced by as much. The effect of emissivity is found to be more pronounced for a thicker medium which has a higher optical thickness. The total heat flux decreases with decrease in ε_w.

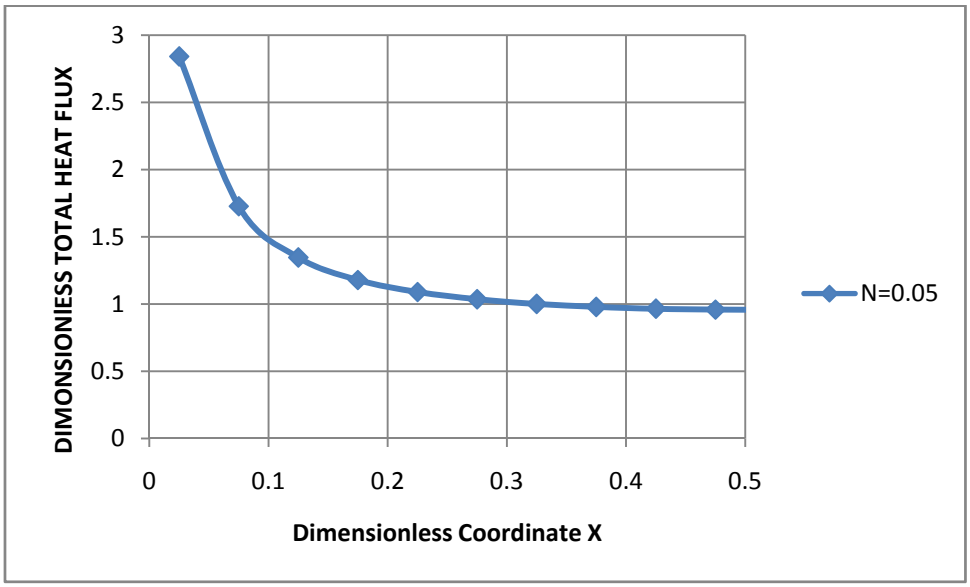

Figure 5.13 Variation of the total heat flux for ε_w=1 at the bottom wall, Y=0

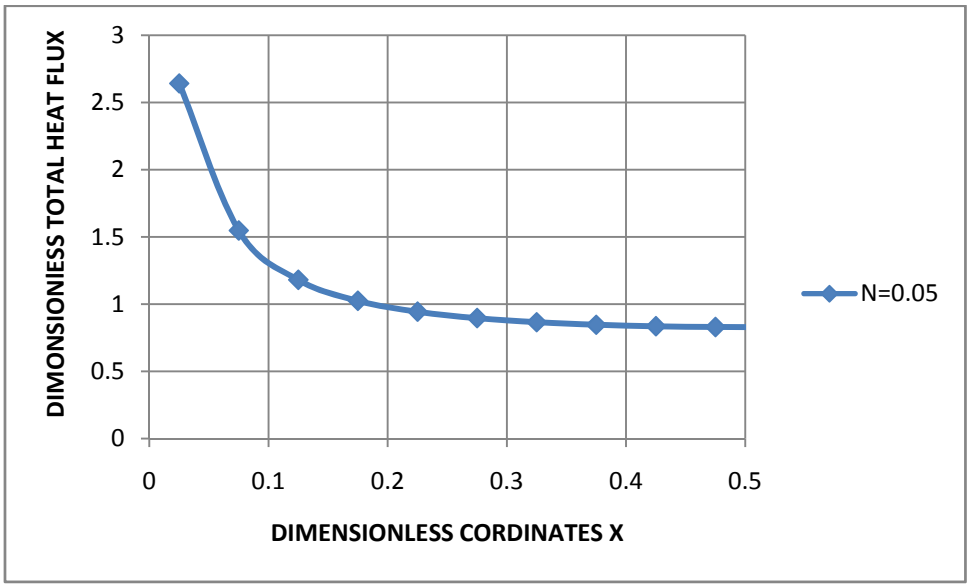

Figure 5.14 Variation of the total heat flux for ε_w=0.8, at the bottom wall, Y=0.

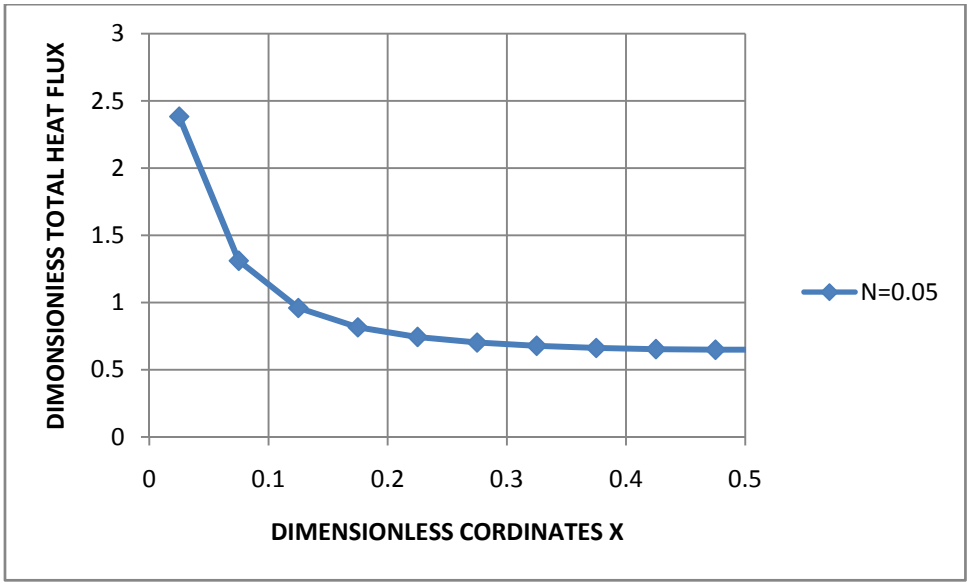

Figure 5.15 Variation of total heat flux for ε_w=0.5, at the bottom wall, Y=0.

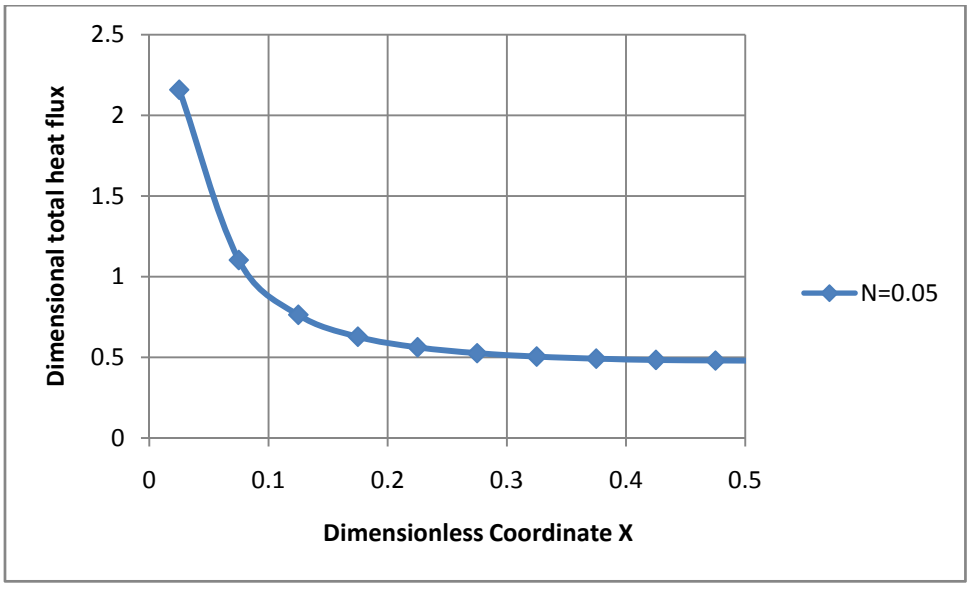

Figure 5.16 Variation of total heat flux for ε_w=0.2, at the bottom wall, Y=0.

5.5 Temperature Isotherms for different scattering albedo and emissivity at steady state conditions: The figures shown below are the temperature isotherms at steady state. In all the cases the conduction-radiation parameter N=0.001 is taken, that makes the phenomena as radiation dominant. Fig.5.17 shows the medium is non-scattering, therefore the last isotherm is formed very close to the top cold wall.

Fig.5.18 shows the medium is absorbing and scattering. The isotherms at the lower-left-hand corner are less steep.

Fig.5.19 shows the medium is purely scattering. It takes more time to reach at the steady state. The isotherms are similar to the isotherms obtained for conduction, fig.(5.1).

Fig.5.20 shows the medium is non-scattering and wall emissivity of ε_w=0.5. As the wall emissivity increases, the intensity at the hot wall increases and it further increases the radiative heat flux and the temperature of the medium inside. Thus the last isotherm is very closer to the top cold wall.

Fig.5.21 shows the medium is scattering with ω=0.5 and wall emissivity ε_w=0.5. The combined effect takes more time to reach at the steady state.

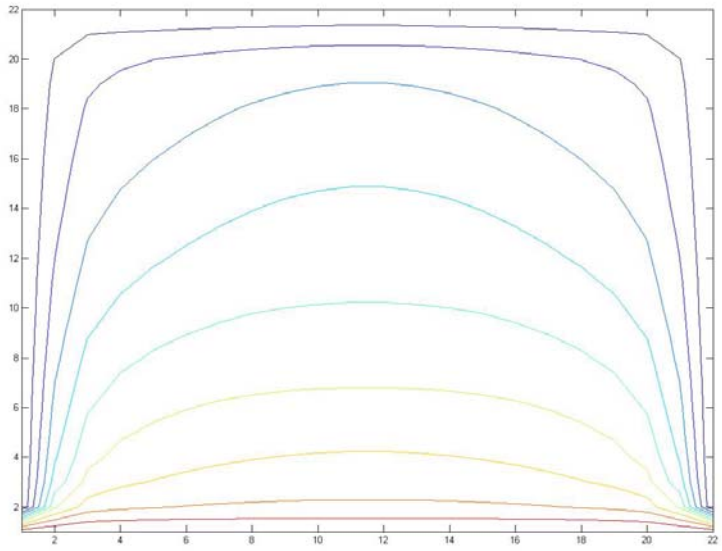

Figure 5.17 Temperature isotherms for N=0.001 and ω=0.

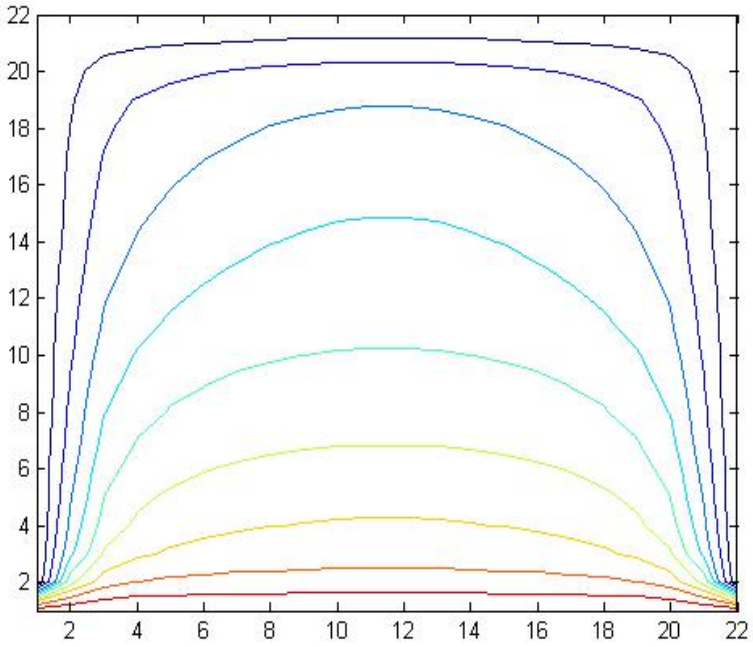

Figure 5.18 Temperature isotherms for N=0.001 and ω=0.5.

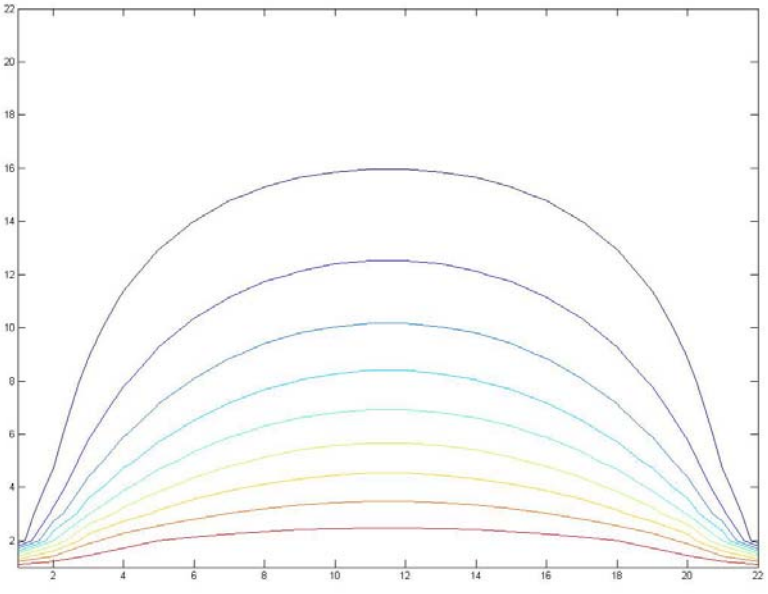

Figure 5.19 Temperature isotherms for N=0.001 and ω=1.

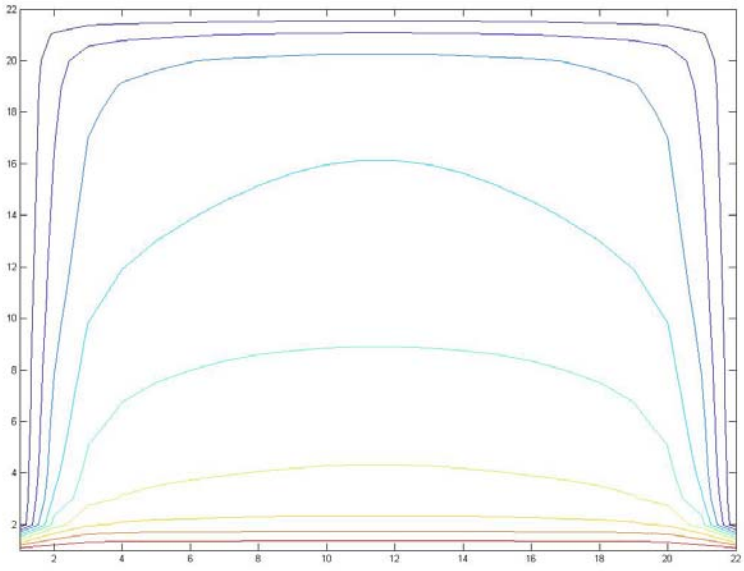

Figure 5.20 Temperature isotherms for N=0.001 and ω=0 and ε=0.5.

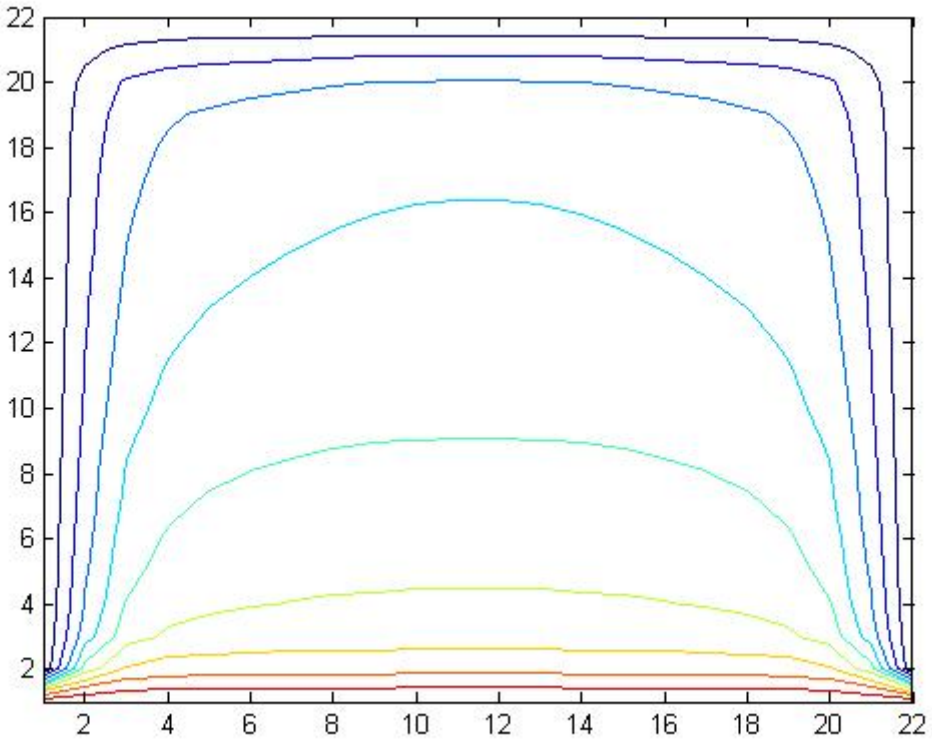

Figure 5.21 Temperature isotherms for N=0.001 and ω=0.5 and ε=0.5.

5.6 COMPARISION OF ISOTHERMS AT DIFFERENT TIME STEPS:

Temperature isotherms at different time step for N=0.001 and ω=0.5 and ε=0.5 are shown below.

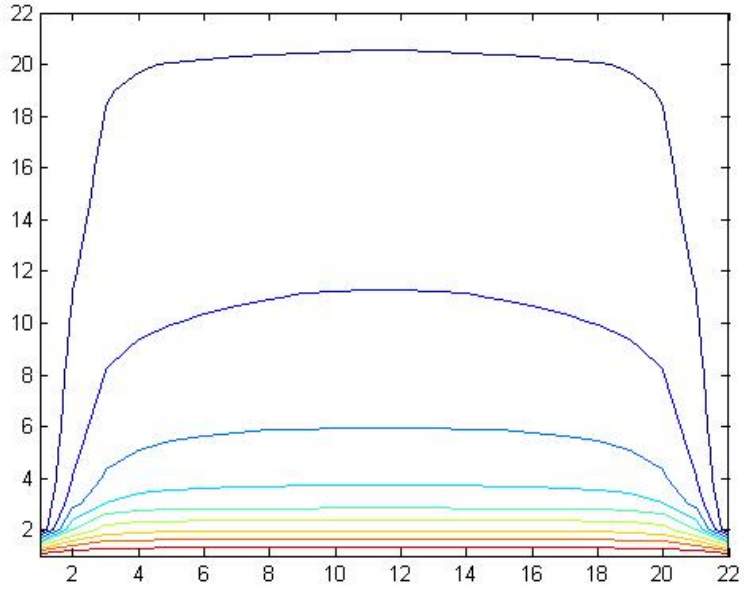

Figure 5.22 Number of time steps = 20.

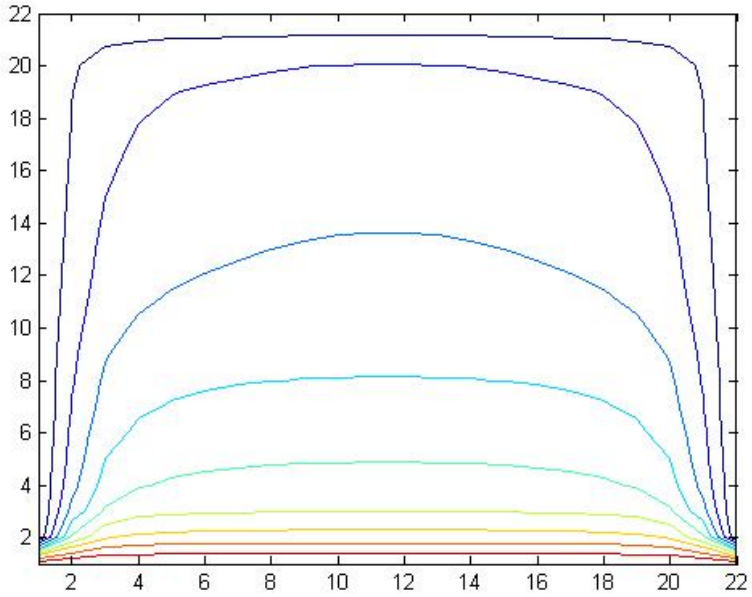

Figure 5.23 No of time steps=40.

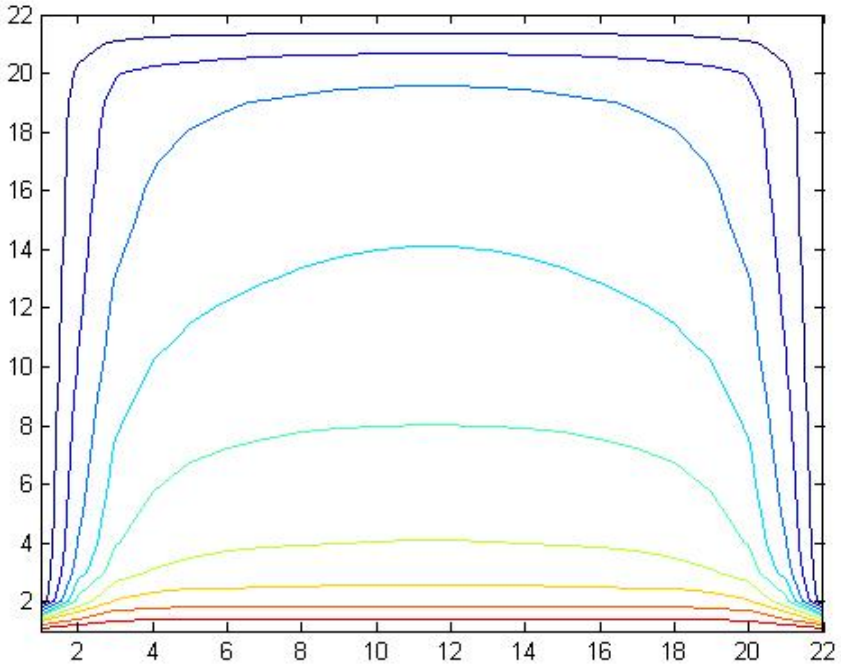

Figure 5.24 No of time steps=80.

5.6.1 Transient Results of temperature: The figure shown below, describes the temperature variations at different time steps, for N=0.001, ω=0.5 and ε=0.5 at the mid plane. The physical time required to reach at the steady state can be calculated.

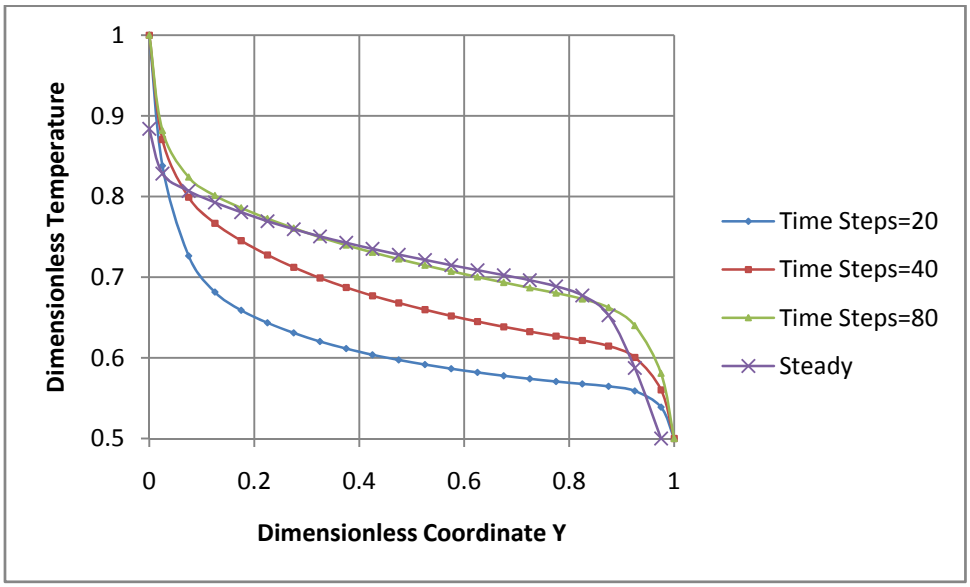

Figure 5.25 Temperature Variation with time at the mid plane

Table 5.1 shows variation in time period required to reach at steady state

Fixed parameters	Varying parameters		No. of time steps
N=0.001 ε=1 τ=1	ω	0	117
		0.5	163
		1	1877
ε=1 τ=1 ω=0	N	1	1851
		0.1	1606
		0.01	624
		0.001	117
N=0.001 τ=1 ω=0	ε_w	0.2	229
		0.5	148
		0.8	124
		1	117

Time required to reach at steady state conditions depends upon ω, ε , and τ, all the radiative properties and conduction-radiation parameter N. As the value of N decreases the phenomena will be radiation dominant, thus the period of transient is small. As the emissivity of the wall increases, the period of transient decreases. As the scattering albedo ω increases the period of transient increases.

CHAPTER 6

CONCLUSIONS

6.1 CONCLUSIONS

Application of the FVM was extended to the solution of the energy equation of a radiation and Fourier heat conduction problem. The FVM was used to compute the radiative information. Combined conduction radiation problems with mixed boundary condition problems were studied. Results of the present work were validated against those available in the literature. Good agreements were found. Temperature distributions in the medium were analyzed for different values of the conduction radiation parameter. The results for the temperature distribution and isothermal contours were illustrated. Additionally fractional radiative heat flux and total heat flux were also introduced and discussed. The results of the temperature distribution at different time step were illustrated. Conclusively the finite volume method is considered to be highly integrable with other finite differenced transport equations. Furthermore it was found that only a reasonably short computational time was required to yield quite accurate solutions.

6.2 FUTURE SCOPE

[1] Analysis of non-Fourier conduction-radiation heat transfer in a 2-D and 3-D systems.
[2] Analysis of non-Fourier heat conduction-radiation heat transfer in cylindrical and spherical system using FVM.
[3] CLAM scheme can be used to solve the radiative transfer equation by FVM.
[4] Convection phenomenon can be added with different boundary condition to the problem.

REFERENCES

REFERENCE

1. R. Viskanta and R. J. Grosh, Heat Transfer by Simultanous Conduction and Radiation in an Absorbing Medium, *J. Heat Transfer*, vol. 84, no. 1, pp. 63-72, 1962.
2. R. Viskanta, Heat Transfer by Conduction and Radiation in Absorbing and Scattering Materials, *J. Heat Transfer*, vol. 87, no. 1, pp. 143-150, 1965.
3. W. W. Yuen and L. W. Wong, Heat Transfer by Conduction and Radiation in a One-Dimensional Absorbing, Emitting and Anisotropically-Scattering Medium, *J. Heat Transfer*, vol. 102, no. 2, pp. 303-307, 1980.
4. P. Talukdar and Subhash C. Mishra, Analysis of Conduction-Radiation Problem in Absorbing-Emitting Media Using Collapsed Dimension Method, in *34th National Heat Transfer Conference Pittsburgh, PA*, paper no. NHTC2000-12129, 2000.
5. P. Talukdar and Subhash C. Mishra, Analysis of Conduction-Radiation Problem in Absorbing, Emitting and Anisotropically Scattering Media Using Collapsed Dimension Method, *Int. J. Heat Mass Transfer*, submitted.
6. C. C. Lii and M. N. Ozisik, Transient Radiation and Conduction in an Absorbing, Emitting, Scattering Slab with Re£ective Boundaries, *Int. J. Heat Mass Transfer*, vol. 15, no. 5, pp. 1175-1179 , 1972.
7. C. Barker and W. H. Sutton, The Transient Radiation and Conduction Heat Transfer in a Gray Participating Medium with Semi-Transparent Boundaries, in *ASME Radiation Heat Transfer*, vol. HTD-49, pp. 25-36, B. F. Armaly and A. F. Emery, eds., 1985.
8. W. H. Sutton, A Short Time Solution for Coupled Conduction and Radiation in a Participating Slab Geometry, *J. Heat Transfer*, vol. 108, no. 2, pp. 465-466, 1986.
9. J. R. Tsai and M. N. Ozisik, Transient, Combined Conduction and Radiation in an Absorbing, Emitting and Isotropically Scattering Solid Sphere, *Journal of Quant. Spectros. Radiat. Transfer*, vol. 38, no. 4, pp. 243-251, 1987.
10. R. Siegel, Finite Difference Solution for Transient Cooling of a Radiating-Conducting Semitransparent Layer, *J. Thermophys. Heat Transfer*, vol. 6, no. 1, pp. 77-83, 1992.
11. Chengcai Yao and B. T. F. Chung, Transient Heat Transfer in a Scattering-Radiating-Conducting Layer, *J. Thermophys. Heat Transfer*, vol. 13, no. 1, pp. 19-24, 1999.
12. H. Tan, L. Ruan, X. Xia, Q. Yu, and T. W. Tong, Transient Coupled Radiative and Conductive Heat Transfer in an Absorbing, Emitting and Scattering Medium, *Int. J.Heat Mass Transfer*, vol. 42, pp. 2967-2980, 1999.

13. H. Tan and M. Lallemand, Transient Radiative-Conductive Heat Transfer in Flat Glasses Submitted to Temperature, Flux and Mixed Boundary Conditions, *Int. J. Heat Mass Transfer*, vol. 32, no. 5, pp. 795-810, 1989.
14. W. W. Yuen and M. Khatami, Transient Radiative Heating of an Absorbing, Emitting and Scattering Material, *J. Thermophys. Heat Transfer*, vol. 4, no. 2, pp. 193-198, 1990.
15. J. H. Tsai and J. D. Lin, Transient Combined Conduction and Radiation with Anisotropic Scattering, *J. Thermophys. Heat Transfer*, vol. 4, no. 1, pp. 92-97, 1990.
16. T. W. Tong, D. L. McElroy, and D. W. Yarbrough, Conduction and Radiation Heat Transfer in Porous Thermal Insulations, *J. Thermal Insulation*, vol. 9, pp. 13-29, 1985.
17. S. W. Baek, T. Y.Kim, and J. S. Lee, Transient Cooling of a Finite Cylindrical ediumin a Rarefied Cold Environment, *Int. J. Heat Mass Transfer*, vol. 36, no. 16, pp. 3949-3956,1993.
18. C. F. Tsai and G. Nixon, Transient Temperature Distribution of a Multilayer Composite Wall with Effects of Internal Thermal Radiation and Conduction, *Numer. Heat Transfer*, vol. 10, no. 1, pp. 95-101, 1986.
19. O. Hahn, F. Raether, M. C. Arduini-Schuster, and J. Fricke, Transient Coupled Conductive/Radiative Heat Transfer in Absorbing, Emitting and Scattering Media:Application to Laser-Flash Measurements on Ceramic Materials, *Int. J. Heat Mass Transfer*, vol. 40, no. 3, pp. 689-698, 1997.
20. L. A. Diaz and R. Viskanta, Experiments and Analysis on the Melting of a Semi-Transparent Material by Radiation, *Warme-und Stoffubertragung*, vol. 20, no.4, pp. 311-321, 1986.
21. M. Nishimura, Y. Bando, M. Kuraishi, and E. W. P. Hahne, Direct Storage of Solar Thermal Energy Using a Semi-Transparent PCM-Indoor Experiments under Constant Incidence of Radiation, *Int. Chemical Engineering*, vol. 29, no. 4, pp. 722-728, 1989.
22. L. K.Matthews, R. Viskanta, and F. P. Incropera, Combined Conduction and Radiation Heat Transfer in Porous Materials Heated by Intense Solar Radiation, *J. Solar Energy Engineering* , vol. 107, no. 1, pp. 29-34, 1985.
23. M. N. Ozisik, *Radiative Transfer*. Wiley, New York (1973).
24. J.R. Howell, Application of Monte-Carlo to heat transfer problem. In *Advances in Heat Transfer* (Edited by T.F Irvine and J.P Hartnett) , Vol. 5, pp. 54, Academic Press, New York (1968).

25. J.J. Noble, The Zone method: explicit matrix relations for total exchange areas, *Int. J. Heat Mass Transfer* 18, 261-269(1975).
26. M.M Razzaque, J.R. Howell and D.E Klein, Coupled radiative and conductive heat transfer in a two-dimensional rectangular enclosure with gray participating media using finite elements. *J. Heat Transfer* 106, 613-619(1984).
27. Raithby, G.D., and Chui, E.H., A finite-Volume Method for predicting a Radiant Heat Transfer in Enclosures with Participating Media," *Journal of Heat Transfer,* Vol. 112, No. 2, 1990, pp. 415-423.
28. Chui, E.H., Raithby, G.D., and Huges, P.M.J., "Prediction of Radiative Transfer in Cylinderical Enclosures with the Finite-Volume Method," *Journal of Thermophysics and Heat Transfer,* Vol. 6, No. 4, 1992, pp. 605-611.
29. Chui, E.H., and Raithby, G.D., "Computation of Radiant Heat Transfer on a Nonorthogonal Mesh Using the Finite-Volume Method," *Numerical Heat Transfer,* Vol.23, Pt. B, 1993, pp. 269-288.
30. Chai, J.C., Lee, H.S., and Patankar, S.V., "Improved Treatment of Scattering Using the Discrete Ordinates Method," *Journal of Heat Transfer,* Vol. 116, No.1, 1994, pp. 260-263.